Journal of Visualized Experiments

Characterizing Individual Protein Aggregates by Infrared Nanospectroscopy and Atomic Force Microscopy

--Manuscript Draft--

Article Type:	Invited Methods Article - JoVE Produced Video
Manuscript Number:	JoVE60108R1
Full Title:	Characterizing Individual Protein Aggregates by Infrared Nanospectroscopy and Atomic Force Microscopy
Keywords:	Amyloid, Neurodegeneration, Protein Aggregation, Atomic Force Microscopy, Infrared Nanospectroscopy, Single Molecule Analysis, Spectroscopy.
Corresponding Author:	F Dr. Ruggeri
Corresponding Author's Institution:	
Corresponding Author E-Mail:	fsr26@cam.ac.uk
Order of Authors:	Francesco Simone Ruggeri
	Tomas Šneideris
	Sean Chia
	Michele Vendruscolo
	Tuomas P. J. Knowles
Additional Information:	
Question	**Response**
Please indicate whether this article will be Standard Access or Open Access.	Standard Access (US$2,400)
Please indicate the **city, state/province, and country** where this article will be **filmed**. Please do not use abbreviations.	Department of Chemistry, University of Cambridge, United Kingdom

TITLE:

Characterizing Individual Protein Aggregates by Infrared Nanospectroscopy and Atomic Force Microscopy

AUTHORS AND AFFILIATIONS:

Francesco Simone Ruggeri[1], Tomas Šneideris[1,2], Sean Chia[1], Michele Vendruscolo[1], Tuomas P. J. Knowles[1,3]

[1]Centre for Misfolding Diseases, Department of Chemistry, University of Cambridge, Cambridge, UK
[2]Institute of Biotechnology, Life Sciences Center, Vilnius University, Vilnius, Lithuania
[3]Cavendish Laboratory, Department of Physics, University of Cambridge, Cambridge, UK

Email addresses of co-authors:

Tomas Šneideris	(sneideris.t@gmail.com)
Sean Chia	(skrc2@cam.ac.uk)
Michele Vendruscolo	(mv245@cam.ac.uk)

Corresponding authors:

Francesco Simone Ruggeri	(fsr26@cam.ac.uk)
Tuomas P. J. Knowles	(tpjk2@cam.ac.uk)

KEYWORDS:

amyloid, neurodegeneration, protein aggregation, atomic force microscopy, infrared nanospectroscopy, single molecule analysis, spectroscopy

SUMMARY:

We describe the application of infrared nanospectroscopy and high-resolution atomic force microscopy to visualize the process of protein self-assembly into oligomeric aggregates and amyloid fibrils, which is closely associated with the onset and development of a wide range of human neurodegenerative disorders.

ABSTRACT:

The phenomenon of protein misfolding and aggregation results in the formation of highly heterogeneous protein aggregates, which are associated with neurodegenerative conditions such as Alzheimer's and Parkinson's diseases. In particular low molecular weight aggregates, amyloid oligomers, have been shown to possess generic cytotoxic properties and are implicated as neurotoxins in many forms of dementia. We illustrate the use of methods based on atomic force microscopy (AFM) to address the challenging task of characterizing the morphological, structural and chemical properties of these aggregates, which are difficult to study using conventional structural methods or bulk biophysical methods because of their heterogeneity and transient nature. Scanning probe microscopy approaches are now capable of investigating the morphology of amyloid aggregates with sub-nanometer resolution. We show here that infrared (IR) nanospectroscopy (AFM-IR), which simultaneously exploits the high resolution of AFM and

the chemical recognition power of IR spectroscopy, can go further and enable the characterization of the structural properties of individual protein aggregates, and thus offer insights into the aggregation mechanisms. Since the approach that we describe can be applied also to the investigations of the interactions of protein assemblies with small molecules and antibodies, it can deliver fundamental information to develop new therapeutic compounds to diagnose or treat neurodegenerative disorders.

INTRODUCTION:

Over 40 million people worldwide are currently affected by neurodegenerative disorders, such as Alzheimer's (AD)[1] and Parkinson's (PD)[2] diseases. More generally, more than fifty pathologies are associated at the molecular level with protein misfolding and aggregation, a process that leads to the proliferation of insoluble fibrillar protein aggregates, known as amyloid deposits[3,4]. The molecular origins of neurodegeneration and its links with protein conformational changes of proteins leading to amyloid formation, however, remain unclear, in large part because of the high level of heterogeneity, transient nature and nanoscale dimensions of the pathological aggregates[4,5].

Highly successful investigations of protein structures in the last several decades have been based widely on the use of bulk methods, including X-ray crystallography, cryo-electron microscopy and nuclear magnetic resonance spectroscopy[5–9]. Within this class of techniques, infrared (IR) spectroscopy has emerged as a sensitive analytical tool to unravel the chemical properties of biological systems such as proteins[8]. IR methods allow the quantification of protein secondary and quaternary structural changes during their misfolding and aggregation. In addition, in order to further decipher at the microscopic level the mechanistic details involved in the complex free energy landscapes of protein during their aggregation, a major advance has been the development of chemical kinetics tools to extend to complex self-assembly pathways including amyloid fibrils formation[5–7,10–12]. However, bulk spectroscopic methods provide only average information on the heterogeneous ensemble of species present in solution or involved in specific microscopic steps, thus rendering the investigation of the biophysical properties of individual aggregated species challenging at the nanoscale level[13,14].

Several microscopy techniques with the capability of operating on scales smaller than the diffraction limit of light have emerged in the last decades. This class of methods includes electron microscopy (EM) and atomic force microscopy (AFM). While scanning electron microscopy (SEM) and transmission electron microscopy (TEM) provide two-dimensional (2D) images of a specimen, AFM has emerged in the last decades as a powerful and versatile technique to study three-dimensional (3D) morphologies, as well as the nanomechanical properties of a sample with sub-nanometer resolution[13–27]. The rationale behind studying protein aggregation via AFM is that this approach enables the investigation of the morphology of individual species present in solution[13,14,16,17,19–21,25,27–37]. In particular, by monitoring the sample as a function of time, AFM allows the investigation of the evolution of the morphology of the species within the sample, which makes it possible to follow and visualize the pathways of amyloid formation[23,25,38–42]. Furthermore, AFM enables the quantification of structural parameters such as cross-sectional heights and lengths of the individual species present in solution[13,19,30–37,40,43–48]. However, the

study of a single biophysical property, such as morphology, is often not sufficient when studying heterogeneous and complex biological systems. AFM, SEM or TEM imaging methods alone do not readily reveal the chemical properties of heterogeneous species of amyloid aggregates at the nanoscale.

A major advance for the analysis of heterogeneous biological samples at this scale has been made recently with the development and application to the field of protein aggregation of infrared nanospectroscopy (AFM-IR)[24,26,38,42,49–52]. This innovative method exploits the combination of the spatial resolution of AFM (~1−10 nm) with the chemical analysis power of IR. The AFM-IR technique is based on the measurement of the photothermal induced resonance effect driven by an IR laser, and on the measurement of the thermal expansion of the sample under investigation by the AFM tip. The sample can be illuminated by the IR laser directly from the top or from the bottom in total internal reflection, similarly as in conventional infrared spectroscopy[24,42,52,53]. The IR laser can be pulsed with typical frequencies in the order of hundreds of kilohertz (1−1000 kHz) and tuned over a wide spectral range, typically between 1000−3300 cm^{-1}. Although the laser source covers an area of ~30 µm diameter, the spatial resolution of the AFM-IR technique is determined nominally by the AFM tip diameter, which detects the local thermal expansion of the system. AFM-IR is well suited to study biological samples because the IR signal is proportional to their thickness up to 1−1.5 µm, and the resulting IR spectra are generally in agreement with the corresponding FTIR transmission spectra[13,54,55]. For this reason, established methods of analysis in spectroscopy can be readily applied, such as the study of chemical shifts, band shape change and de-convolution by second derivatives analysis[52]. Overall, combining the spatial resolution of AFM with the chemical recognition power of IR spectroscopy, AFM-IR enables the simultaneous acquisition of a wide range of morphological, mechanical and chemical properties of a sample at the nanoscale.

Here, we illustrate a protocol for the characterization of the process of protein aggregation that exploits the combination of in vitro fluorescence assays, high-resolution AFM imaging and nanoscale AFM-IR. This combined approach has already excelled in providing detailed results in studying the chemical and structural properties of individual micro-droplets formed by protein aggregates, in the study of liquid-liquid protein phase separation, and in investigating the heterogeneity and biophysical properties of individual aggregated species at the nanoscale[23,26,38,45,50,53,56,57].

PROTOCOL:

1. Aggregation assays on fluorescence plate readers

NOTE: The protocol described here is an example of how to study the aggregation of any protein or peptide by chemical kinetics. In particular, it describes an optimized protocol to study the aggregation of the Aβ42 peptide, which is involved in the onset and progression of Alzheimer's disease[58,59]. A similar protocol can be adjusted and adopted towards studying the aggregation of any protein or peptide.

1.1. Obtain a highly pure monomeric solution of Aβ42 through ion-exchange and size-exclusion chromatography techniques to distinguish protein fractions containing Aβ42, and to isolate the monomeric fraction from other aggregated forms of Aβ42 obtained[58,59].

1.2. Dilute the Aβ42 peptide in 20 mM sodium phosphate buffer, 200 µM EDTA at pH 8.0[58] to a desired final concentration ranging between 1−5 µM, in 1.5 mL low-bind tubes. Samples collected for AFM measurements should not contain the fluorescent dye used in the aggregation assay (thioflavin T, ThT), as it might introduce artefacts during sample deposition for AFM analysis. Thus, prepare triplicates of two identical solutions: i) the first containing monomeric Aβ42 to follow the process of aggregation by AFM; ii) the second containing the Aβ42 monomeric with addition of 20 µM ThT as a tracer to monitor the kinetics of aggregation.

NOTE: It is important to perform steps 1.1 and 1.2 on ice. This procedure is to ensure that the monomeric Aβ42 solution does not aggregate until initiated in the plate reader. When handling samples, careful pipetting is essential to avoid the introduction of any air bubbles that may affect the protein sample.

1.3. Pipette 80 µL of each sample in each well of a 96-well, half-area plate of black polystyrene with clear bottom and nonbinding surfaces.

1.4. Seal the plate with a foil to minimize the evaporation of the sample over the course of the aggregation.

1.5. Equilibrate the temperature of the plate reader to 37 °C.

1.6. Set up the aggregation protocol to read fluorescence measurements at fixed time-point intervals, at an excitation wavelength of 440 nm and an emission wavelength of 480 nm. The aggregation should be initiated in quiescent conditions.

1.7. Insert the plate into the plate reader.

NOTE: It is important to be careful while handling the plate, to ensure that the aggregation is not triggered prior to starting the plate reader. Use the gain adjustment settings to ensure the optimal readout of the fluorescence of each sample.

1.8. Start the measurement.

NOTE: The aggregation experiment is concluded when the ThT fluorescence sigmoidal curve reaches a plateau[58].

2. Sample preparation for AFM and nano-IR measurements

2.1. Glue highest quality grade V1 mica disc to high quality magnetic stainless-steel disc using adhesive tabs or double-sided tape.

2.2. Etch mica by placing a piece of adhesive tape onto the mica surface and pulling off the top layer of the mica. This procedure will produce clean, atomically flat surface, suitable for sample deposition.

NOTE: Etched surface must be uniform and smooth.

CAUTION: Do not touch or breathe directly above freshly etched mica, as this will introduce artefacts.

2.3. Pause/stop the plate reader measurement to collect the time point of interest during the aggregation process of the protein.

2.4. Remove the sealing foil and collect 10 µL aliquot of the samples without ThT from the well into a 1.5 mL low-bind tubes.

2.5. Deposit the 10 µL of the sample on the freshly etched mica. For AFM-IR measurements samples must be deposited on freshly stripped gold substrate.

2.6. Incubate the solution on the mica for 1 min to allow physisorbtion.

NOTE: Longer incubation time would allow better absorption on the surface but may induce artificial self-organization and self-assembly[25]. To avoid these effects, spray deposition may be exploited[25].

2.7. Rinse three times with 1 mL of ultrapure water.

2.8. Dry under a gentle flow of nitrogen to measure the sample in air environment.

3. AFM imaging of the morphology of protein aggregates

NOTE: Morphology measurements can be performed both in contact and dynamic mode, in the following steps the latter is described since it reduces lateral forces to measure the 3D morphology of the sample with high resolution. AFM-IR measurements will be performed in contact mode to enhance AFM-IR signal-to-noise ratio.

3.1. Turn on the AFM system at least 30 min before the measurements in order to enable the system to reach thermal stability. Click on **Setup**, then on **Probe**. In **Probe Change** window click on **Next** to prepare **Z, Focus Stage**.

3.2. Turn off the AFM beam switch (if it is on). Unlock the dovetail locks, disconnect the head from the system and in **Probe Change** window click on **Next**.

3.3. Mount the AFM cantilever on the probe holder. Connect the head to the system and lock the

dovetail locks.

NOTE: Optimal cantilevers to study biological samples in dynamic mode AFM have spring constant ranging between 2–40 N m^{-1} and an apex radii ranging between 2–8 nm[14].

3.4. Turn on the AFM laser beam switch and in **Probe Change** window click on **Next**.

3.5. In the pop-up window click on **No** if the cantilever type did not change. Adjust optical alignment knobs to find the cantilever. Adjust focus onto cantilever and click on **Next**.

3.6. In the pop-up window click on **Yes** if the focus is on the cantilever.

3.7. Position the laser beam at the end of the cantilever using the knobs controlling position of the detection laser. Maximize the total signal measured by the four-quadrant photodiode to at least >1 V using the knobs controlling the position of the deflected laser beam on the position sensitive photodiode (PSPD). In **Probe Change** window click on **Next** and then on **Close**.

3.8. Wait 15 min for the cantilever to reach thermal stability. Readjust the position of the deflected laser beam on the PSPD if necessary.

3.9. Click on **NCM SWEEP**, choose desired amplitude of oscillation, click on **Use Phase**, click on **auto** and tune the cantilever close to the maximum of its first free resonance of oscillation, which is of approximately 300 kHz for a cantilever with a spring constant of 40 N m^{-1}.

NOTE: Tuning the cantilever out of the maximum of its free resonance assures higher stability of the measurements[14].

3.10. Place the sample on the sample holder. Choose suitable imaging parameters. Typical scanning rate is 0.3–1.0 Hz for a scan area of 1 x 1 μm^2 to 5 x 5 μm^2. Typical resolution needed is between 256 x 256 and 1024 x 1024 pixels. Click on **Scan Area** to choose the scan size and the pixel number.

3.11. Focus the optical view on the sample. Click on **Approach** to approach the sample surface. Once approach is completed click on **Lift 100 µm** to rise the AFM tip 100 µm above the surface of the sample. Click **Expand** on the optical image of the sample. Click on the **Focus Stage** bar to focus the view on the surface of the sample.

3.12. Use the arrows to move in the region of the sample of interest. Engage the surface by pressing **Approach** button. Click on **Line Scan** button, and check if the tip is following the surface well, if necessary, adjust the **Set Point**.

3.13. Start imaging the sample surface by pressing **Scan** button. During imaging, to avoid large imaging force and keep consistency of within independent samples, maintain a constant regime of phase change not exceeding Δ20°[42].

3.14. Enter file name and choose base directory where the acquired image will be saved.

4. Infrared nanospectroscopy measurements of protein aggregates

4.1. Turn on the AFM-IR system and the infrared (IR) laser[60] 30–60 min before measurements for thermal stabilization. Typical lasers for AFM-IR instruments are optical parameter oscillators (OPO) and quantum cascade lasers (QCL).

4.2. Open the built-in software to control the instrument. Click on **file** and then on **new** to open a new **nanoIR** file. Press the button **initialise** to start the AFM-IR system.

4.3. Open the instrument cover and mount on the AFM-IR system a silicon gold coated probe with a nominal radius of 30 nm and a spring constant of 0.2 N/m to measure the sample in contact mode.

4.4. Click on **Load** in the section **AFM probe** and then **next**. In **focus on probe** section click on the arrows to focus the camera on the cantilever. In the section **sample XY movement**, use the arrows to place the cross-air at the end of the cantilever.

4.5. Rotate the knobs controlling the position of the detection laser to position laser at the end of the cantilever. Rotate the **laser** knobs to detect and maximize the sum measured by the four-quadrant photodiode to a value >3 V. Rotate the **deflection** knob to adjust the cantilever deflection to -1 V and then click **next**. Close the cover of the instrument.

4.6. In the section **focus on sample** use the arrows to focus the camera on the sample. Then, in the section **sample XY movement** use the arrows to move in the region of interest of the sample and click on **approach and engage**.

4.7. In the **microscope** window select as inputs the channels of interest to map the biophysical properties of the sample. In particular, choose **height** for morphology, **Amplitude 2** for IR absorption and **PLL frequency** to map tip-sample contact resonance.

4.8. In the **AFM scan** section of the **controls** window, use similar parameters as in section 3 (i.e., scan rate 0.1–1.0 Hz, between 256 x 256 and 1024 x 1024 pixels). Choose as value of the gains according to sample roughness: integral I = 1–10 and proportional P = 10–30. Then, click on **scan** to acquire a morphology map.

NOTE: The morphology can be similarly measured in the dynamic tapping mode, but AFM-IR measurements are performed here in the contact mode to have higher signal to noise ratios.

4.9. After the mapping of morphology is finished, in the **microscope** window, click on the height map to position the probe on the top of one aggregate. Then in the **nanoIR** section of the **controls** window, click on **start IR** to illuminate the sample with the IR laser.

4.10. To focus the infrared laser on the cantilever, click on **optimisation**. In this window, write a wavenumber where the sample is going to have high absorbance and click **add**. For protein, a typical value is 1655 cm^{-1}. Click on **scan** to find the IR laser position and click on **update** to align its position with the cantilever. Close the window.

4.11. In the section **general** of the **nanoIR** setting, write a wavenumber where high absorbance in the relative field is expected. Then, deactivate the **Band Pass Filter** option and look at the **meter** reading and at the fast Fourier transform (FFT) of the cantilever response. In the FFT window move the green cursor to read the resonance frequency of the cantilever. A typical value of the FFT of the resonance of the cantilevers is around 300 kHz. Write this resonance frequency value in the **general** section in the **freq. centre** field and use a **freq. window** of 50 kHz.

NOTE: Select a laser power that is low enough to not saturate the **meter** reading and to have distortion in the cantilever response and to not overheat the sample.

4.12. Click on **laser pulse tune window** to use the resonance enhanced mode. Choose a frequency centre of 300 kHz, a tune range of 50 kHz and a duty cycle of the laser of 5%. Click on **acquire** to sweep the pulse rate of the laser. By using the cursor in the graph, tune the laser pulse to the frequency of the mechanical response of the thermal expansion of the sample absorbing the IR light. Then, select the option PLL to monitor the contact resonance between the sample and the tip. Press the **zero** button in the PLL window and tick **enable** to track the sample-tip contact resonance. Choose an integral gain I = 0.5 and proportional gain P = 10. Close the window.

4.13. Open again the **optimisation** window and find the position of the IR laser for at least 3 wavenumbers corresponding to major absorbance bands of the sample (amide band I-II-III) and for at least one wavenumber for each chip of the laser.

4.14. Click on **Tools** | **IR Background Calibration** | **New**. In the window select the spectroscopic region of interest (1800−1200 cm^{-1} to study protein samples); choose the same pulse rate as determined in step 4.12 and a duty cycle of 5%; click on **fast** acquisition and select the laser speed, typical range for a quantum cascade laser is between 20−500 cm^{-1}. Click on **acquire** to measure the IR laser background. This background spectrum will be used for normalization of measured nanoscale localized spectra. Close the window.

NOTE: If a fast laser and resonance enhanced mode is not available, skip step 4.12 and select **stepped** spectra instead of **fast** in both the **background** and **IR spectra** acquisition windows. However, single aggregate sensitivity will not be reached.

4.15. In the **IR spectra** settings, choose an IR spectrum resolution between 1−4 cm^{-1} and a number of co-averages of at least 64x. Click on **acquire** to measure a nanoscale localized IR spectrum in the protein range (1800−1200 cm^{-1}).

4.16. To acquire a nanoscale resolved chemical map, select **IR imaging** option, choose a

wavenumber of interest (e.g., 1655 cm^{-1} for amide band I) and click on **scan** in the **AFM scan** window.

4.17. Once the mapping is completed, go to **file** and **save** the measurements. To analyze the acquired maps of morphology, contact-resonance and chemistry, as well as the nanoscale localized spectra, use the built-in AFM image processing software. Spectra and Images can be saved as .csv or .axz files for further detailed analysis with commercial software.

5. Image processing and analysis of cross-sectional dimensions

5.1. Flatten raw images[14,17,19,41,42,59] using built-in AFM image processing software or commercial software.

NOTE: The aggregates should be masked from the calculation to avoid artefacts of analysis and underestimation of their measured height.

5.2. Flatten the image by 0 order plane fit subtraction.

5.3. Flatten the image by plane and then line by line at a 1st regression order, the second step is repeated until the flat baseline in line profile of the image is reached.

5.4. If the sample is very crowded, contains exceptionally high aggregates or scanner bow artefact is present, flatten image using 2nd regression order fit.

5.5. Measure aggregate height and width from a line profile taken perpendicular to the fibril axis[14,17,19,41,42,59].

5.6. Measure fibril length parallel to the fibril axis[14,17,19,41,42,59].

REPRESENTATIVE RESULTS:

A representative time course of Aβ42 aggregation, as measured by the ThT fluorescence assay, is shown in **Figure 1**. The aggregation process is commonly characterized by a sigmoidal curve, where a lag phase is initially observed, and is followed by a steep growth phase, before the curve reaches a plateau when an equilibrium steady state is reached[6,7,58]. It is essential to ensure that an optimized aggregation protocol is used to generate high-quality data to study the molecular details pertaining to aggregation processes[58].

High resolution of AFM enables to investigate the morphology and heterogeneity of the aggregated species at different time points of the process. During the aggregation, monitored by the ThT assay, aliquots of the sample in the plates are prepared for single aggregate investigation by AFM and nano-IR (**Figure 1**). The typical process flow of manual sample preparation is shown in **Figure 2**. At the completion of the measurement of the 3D morphology of the sample by high resolution and phase-controlled AFM, the maps are flattened to remove non-linearity of the piezoelectric scanner and reduce sources of error in post-processing analysis of sample

morphology (**Figure 3**). Subsequently, an accurate and sensitive single molecule statistical analysis can be performed, as shown in **Figure 4**. From a 3D morphology map, it is possible to extract aggregate cross-sectional height, width and length (or diameter in case of spheroidal particles), which allows to distinguish and characterize distinct species of aggregates present during the aggregation time course[23,38]. Typical time points of interest to investigate the process of aggregation are the lag phase, the growth phase and the plateau phase (**Figure 1**). During the lag phase, monomeric and oligomeric species of Aβ42 are primarily present. When visualized by AFM, monomeric and oligomeric species of Aβ42 typically appear as spheroidal particles 1−15 nm in diameter and 0.3−2 nm in height (**Figure 1, bottom left**)[38,39]. Formation of elongated protofilaments, protofibrils and fibrils is visible during the growth phase of Aβ42 aggregation time course (**Figure 1, bottom middle**)[38,39]. Typically, protofilaments appear as elongated features hundreds of nanometers in length and 0.5−2 nm in height, while protofibrils appear as elongated linear or curvilinear aggregates 1−5 nm in height and hundreds of nanometers in length[38,39]. During the plateau phase, fibrils are the dominant species of Aβ42 aggregates. Aβ42 fibrils typically appear as unbranched, thread-like structures, with a cross-sectional diameter of 6−10 nm and length in the order if micrometers (**Figure 3, bottom right**)[38,39]. Remarkably, this schematic representation of the morphological properties of the aggregates is a general feature of most aggregating proteins and peptides[13,14].

After the investigation of the sample morphology, nano-IR can be used to investigate the chemical properties of the individual protein aggregate species present during the process of aggregation, by acquiring nanoscale-resolved IR maps and spectra both in air and native liquid environment[24,26,38,42,49–52]. **Figure 5** shows a schematic illustration of the AFM-IR setup. An IR source is used to illuminate the sample from the bottom in total internal reflection or directly from the top as in **Figure 5a**. If the IR light is absorbed by the sample, it will excite the corresponding molecular vibrational energy transition levels of the species present. The vibrational energy is dissipated inside the sample in the form of thermal heating, which causes the thermal expansion of the sample. This expansion is measured at the nanoscale by the AFM tip in contact with the sample with a resolution in the order of 10 nm. At each pulse, the cantilever detects the thermal expansion. In particular, the fast expansion of the sample kicks out the cantilever from contact with the sample, and after the kick out the cantilever rings down at its natural frequencies. In order to enhance the sensitivity of AFM-IR, it is possible to tune the laser pulse frequency at the same frequency of the oscillation of the cantilever[54]. In order to work in this resonance-enhanced mode, it is necessary to have IR sources that can be pulsed in a wide range of frequencies, such as quantum cascade lasers that operate typically in a range between 1−1000 kHz. The peak-to-peak amplitude and the fast Fourier transform of the ringdown signal, termed IR amplitude, of the raw cantilever deflection are proportional to the IR light absorbed. These signals are detected in real time by measuring the deflection of a red laser focused on the top of the cantilever. In order to acquire chemical maps, the laser wavenumber is fixed at a certain wavenumber and the IR amplitude signal is collected at each point of the map, while, to acquire IR spectra, the position of the cantilever is fixed in a position of interest and the laser wavelength is swept along the spectroscopic range of interest. The ultimate resolution of AFM-IR enables the measurement of the chemical properties of protein aggregates with a cross-sectional height of approximately 5 nm, as represented in **Figure 6**.

FIGURE LEGENDS:

Figure 1: Monitoring of the aggregation time course in vitro via ThT fluorescence and AFM. Samples taken during the lag phase, growth phase, and plateau phase of the aggregation process as detected by ThT fluorescence were imaged via high-resolution AFM. This figure has been adapted from Ruggeri et al.[38].

Figure 2: Schematic representation of the substrate preparation and sample deposition for AFM measurements. (**A, B**) Mica etching using adhesive tape. (**C**) Sample deposition. (**D**) Sample incubation. (**E**) Sample rinsing with ultrapure water. (**F**) Sample drying under gentle flow of nitrogen. (**G**) Sample imaging using microfabricated AFM cantilever with sharp tip on its end. (**H**) Processed image of amyloid fibrils.

Figure 3: AFM image processing procedure[42]. The top of each panel shows a profile line of the sample surface (red line) illustrated by the corresponding AFM image, while the lower part shows a histogram of the height of all pixels in the image. (**a**) Raw AFM image before image flattening procedure. (**b**) AFM image after the processing procedure using the whole plane flattening. Fibrillar structures (pink color) were masked from the flattening procedure. (**c**) Image processed using line-by-line flattening procedure. (**d**) Final image after the image processing procedure. This figure has been adapted from Ruggeri et al.[42].

Figure 4: Single aggregate statistical analysis of AFM images. (**a**) Example of the tracing of the heights and lengths of fibrillar structures, indicated with 1 and 2. (**b**) Graph with sections of the traced fibrils and their average height. (**c**) Example of a histogram showing the average height of fibrillar structures. (**d**) Graph with normalized profile of the traced fibrils 1 and 2. (**e**) Histogram distribution of the normalized profile height points. This figure has been adapted from Ruggeri et al.[42].

Figure 5: Principle of function of the AFM-IR method. (**a**) Absorbed IR light causes the thermal expansion of the sample, exciting the mechanical resonances of the AFM cantilever in contact with the sample. The amplitude of the cantilever oscillations is proportional to the IR absorption. (**b**) IR absorption maps are obtained scanning the cantilever on the sample while fixing the laser wavelength. (**c**) Tip and sample in contact behave as a system of coupled springs whose resonant frequency increases monotonically with the intrinsic stiffness of the sample[50]. (**d**) Localized spectra are obtained by sweeping the laser wavelength while fixing the position of the AFM cantilever. (**e**) IR spectrum of protein. (**f**) In summary, AFM-IR enables the simultaneous study of morphological, mechanical and chemical properties at the nanoscale[26].

Figure 6: In**frared nanospectroscopy** (**nano-IR**) **of a single amyloid aggregate.** (**a**) AFM morphology map. (**b**) IR absorption map at the laser resonance peak at 1658 cm^{-1}. (**c**) Cross sectional dimensions of the fibril height. (**d**) IR spectra on different positions of the fibrillar structure (marked in panel b with blue circles) and the substrate (marked in panel b with green circles). The average net signal deriving from the aggregate structure (solid black line) was

obtained by subtracting the averaged background signal (solid green line) from the averaged fibril signal (solid blue line). This figure has been adapted from Ruggeri et al.[42].

DISCUSSION:

The first critical step in this protocol is the preparation of monomeric proteins, such as in the case of Aβ42 solution described in steps 1.1 and 1.2. It is essential to initiate the aggregation process from a highly pure, monomeric solution, as the presence of oligomeric or aggregated species may result in poor reproducibility of the aggregation kinetics[58], and induce artefacts in the AFM measurements (e.g., fibrillar species will be evident at the initial stages of the aggregation), which may lead to the misinterpretation of the data. Highly reproducible kinetics data of amyloid formation based on ThT fluorescence assay, in association with the master equation formalism of chemical kinetics[5–7], have allowed to define the Aβ42 aggregation mechanism in terms of its underlying molecular events. Chemical kinetics connects the microscopic steps underlying amyloid formation with their macroscopic manifestations by considering the different ways in which new aggregates can form and grow, which are for instance elongation at the aggregate ends or secondary nucleation on the aggregate surface. However, chemical kinetics by itself does not directly enable the visualization of the possible nucleation phenomena at the nanoscale requiring their combination with single molecule methods.

The second critical step in this protocol is the substrate preparation and sample deposition procedures described in steps 2.2 and 2.6−2.8. To avoid artefacts, the sample must be deposited on a clean, atomically flat surface. Proper etching of the mica is essential to achieve artefact-free, high-resolution in AFM measurements. The sample deposition time is also extremely important, as longer incubation time allows better absorption on the substrate surface. However, it might also induce artificial self-organization and self-assembly[25], which may induce artefacts (e.g., surface-induced aggregate species) that may lead to data misinterpretation. In addition, the mica surface is negatively charged, which means that only positively charged molecules easily absorb on it. If the net charge of the sample is negative, the surface of the mica can be positively functionalized using APTES for a better phisisorption[23]. Microfluidic spray deposition[25] can be exploited to avoid these effects and artefacts and deposit the sample in a single step and artefact-free manner.

The third critical step is the proper setup and the choice of imaging parameters for sample imaging via AFM and AFM-IR described in section 3. The AFM tips used for the sample imaging should be sharp enough (apex radii of 2−8 nm) to achieve high-resolution and minimize convolution effects (broadening of the sample features by the tip)[14], which may induce uncertainties in the image of the sample. The choice of imaging mode, contact or dynamic, is also important. For sample imaging via conventional AFM, the dynamic mode is preferred over the contact mode as the latter mode induces large lateral tip-sample frictional forces that may cause sample damage and introduce artefacts in the measurements (e.g., reduction in the sample height due to nanoindentation)[14,61,62]. Conversely, the contact mode is preferred for the measurements via nano-IR to enhance AFM-IR signal. For measurements in dynamic mode, the cantilever should be tuned just slightly below (tapping mode) or above (non-contact mode) the maximum of its first free resonance of oscillation to assure higher stability of the

measurements[14]. The imaging resolution, which depends on the pixel number and scan area, should be high enough to capture the smallest degree of detail present in a specimen (e.g., 1024 x 1024 pixels for a 4 x 4 μm^2 area)[14,63]. Low imaging resolution can induce distortions and uncertainties in the image of the sample due to the loss of the vertical and lateral information upon digitisation of the signal[14]. The scan rate, used for imaging, should be low enough for the tip to be able to follow surface features properly as well as to have enough time to acquire chemical information[14]. One of the most important imaging parameters is the imaging force. In contact mode, it is fundamental to use a low interaction force to preserve structure of the sample. In dynamic mode, the energy dissipation on the samples should be kept constant in order to consistently compare morphology of distinct samples; consistent imaging of independent samples can be obtained by maintaining a constant regime of a phase change not exceeding Δ20°[14,42]. Large imaging forces should be avoided as they may induce distortions and uncertainties in the sample images.

Thermal drift caused by the expansion and contraction of AFM parts due to thermal fluctuations can induce distortions and artefacts in the image of the sample[64,65]. Drifts in the vertical direction may cause the cantilever to lose track of the surface as well as to crash into the surface, while drifts in the lateral direction usually result in elongation of the surface features and image distortion, which makes it difficult to achieve precise measurements of the sample features. The effect of these thermal drifts can be minimized by accurate temperature control of the laboratory as well as giving enough time (around 30 min) for the system to become stable or by performing fast scans[66–70].

The quality of the nano-IR imaging and spectra collection by AFM-IR can be affected by several factors, of which the most important are: (i) a wrong division of the IR signal on the sample by the IR background, (ii) a large variation of nanomechanical contact between tip and the sample, and (iii) an excessive heating of the sample causing its softening. To correctly divide the IR spectrum of the sample by the collected background, it is crucial that they are collected at the same laser power. Indeed, the spectral line shape of the IR laser background depends on the power of the laser. Then, in order to avoid the influence of the mechanical properties of the sample into the measured chemical information, it is crucial to monitor and track the contact resonance between the sample and the tip during spectra and image acquisition. For spectra acquisition, ideally, it is sufficient to pulse the laser at a fixed contact resonance. However, if the spectrum is acquired on a large spectroscopic range, high intensity peaks could cause strong heating of the sample and its softening, thus changing the tip-sample contact resonance and artificially reducing the IR peak amplitude. For this reason, it is important to track contact resonance during spectra acquisition in order to verify that the spectrum is not affected by excessive heating of the sample.

In conclusion, conventional AFM and nano-IR are capable of investigating with high resolution the morphological, structural and chemical properties of the individual species forming during protein aggregation[24,38]. However, they lack the capability of chemical kinetics to follow their rapid kinetics of formation in native bulk conditions. In order to unravel the conformational changes that protein undergo during their aggregation and misfolding, it is necessary to develop

and apply novel biophysical methods capable of bringing together the capabilities of bulk biophysical methods with the investigation of the heterogeneity and ultrastructural properties of protein aggregation at the nanoscale. This approach represents a fruitful avenue to address the challenge of understanding the problem of protein self-assembly and its role in health and disease. Indeed, single aggregate approaches are capable to unravel and elucidate the molecular mechanisms of protein aggregation polymorphism and formation. This information is central to address the challenge of understanding protein aggregation and its role in the onset and progression of human diseases, as well as understanding their biophysical properties for biotechnology applications.

ACKNOWLEDGMENTS:

The authors thank Swiss National Foundation for Science (SNF) for the financial support (grant number P2ELP2_162116 and P300P2_171219), the Darwin College, Erasmus+ program for the financial support (grant number 2018-1-LT01-KA103-046719-15400-P3) and the research leading to these results has received funding from the European Research Council under the European Union's Seventh Framework Programme (FP7/2007-2013) through the ERC grant PhysProt (agreement number 337969), the Newman Foundation (T.P.J.K.) and The Cambridge Centre for Misfolding Diseases (C.G., M.V., and T.P.J.K.).

DISCLOSURES:

The authors have nothing to disclose.

REFERENCES:

1. Selkoe, D. J., Hardy, J. The amyloid hypothesis of Alzheimer's disease at 25 years. *EMBO Molecular Medicine.* **8**, 595–608, doi:10.15252/emmm.201606210 (2016).

2. Poewe, W. et al. Parkinson disease. *Nature Reviews Disease Primers.* **3**, 1–21, doi:10.1038/nrdp.2017.13 (2017).

3. Chiti, F., Dobson, C. M. Protein misfolding, functional amyloid, and human disease. *Annual Review of Biochemistry.* **75**, 333–66, doi:10.1146/annurev.biochem.75.101304.123901 (2006).

4. Chiti, F., Dobson, C. M. Protein misfolding, amyloid formation, and human disease: A summary of progress over the last decade. *Annual Review of Biochemistry.* **86**, 27–68, doi:10.1146/annurev-biochem-061516-045115 (2017).

5. Knowles, T. P. J., Vendruscolo, M., Dobson, C. M. The amyloid state and its association with protein misfolding diseases. *Nature Reviews Molecular Cell Biology.* **15**, 384–396, doi:10.1038/nrm3810 (2014).

6. Meisl, G. et al. Molecular mechanisms of protein aggregation from global fitting of kinetic models. *Nature Protocols.* **11**, 252–272, doi:10.1038/nprot.2016.010 (2016).

7. Knowles, T. P. J. et al. An analytical solution to the kinetics of breakable filament assembly. *Science.* **326**, 1533–1537, doi:10.1126/science.1178250 (2009).

8. Barth, A. Infrared spectroscopy of proteins. *Biochimica et Biophysica Acta (BBA) - Bioenergetics.* **1767**, 1073–1101, doi:10.1016/j.bbabio.2007.06.004 (2007).

9. Fitzpatrick, A. W. P. et al. Atomic structure and hierarchical assembly of a cross- amyloid fibril. *Proceedings of the National Academy of Sciences of the United States of America.* **110**, 5468–5473, doi:10.1073/pnas.1219476110 (2013).

10. Cohen, S. I. A. et al. Proliferation of amyloid-β42 aggregates occurs through a secondary nucleation mechanism. *Proceedings of the National Academy of Sciences of the United States of America.* **110**, 9758–9763, doi:10.1073/pnas.1218402110 (2013).
11. Michaels, T. C. T., Lazell, H. W., Arosio, P., Knowles, T. P. J. Dynamics of protein aggregation and oligomer formation governed by secondary nucleation. *Journal of Chemical Physics.* **143**, doi:10.1063/1.4927655 (2015).
12. Šarić, A., Michaels, T. C. T., Zaccone, A., Knowles, T. P. J., Frenkel, D. Kinetics of spontaneous filament nucleation via oligomers: Insights from theory and simulation. *The Journal of Chemical Physics.* **145**, 211926, doi:10.1063/1.4965040 (2016).
13. Ruggeri, F. S., Habchi, J., Cerreta, A., Dietler, G. AFM-based single molecule techniques: Unraveling the amyloid pathogenic species. *Current Pharmaceutical Design.* **22**, 3950–3970, doi:10.2174/1381612822666160518141911 (2016).
14. Ruggeri, F. S., Šneideris, T., Vendruscolo, M., Knowles, T. P. J. Atomic force microscopy for single molecule characterisation of protein aggregation. *Archives of Biochemistry and Biophysics.* **664**, 134–148, doi:10.1016/j.abb.2019.02.001 (2019).
15. Iljina, M. et al. Nanobodies raised against monomeric α-synuclein inhibit fibril formation and destabilize toxic oligomeric species. *BMC Biology.* **15**, 1–14, doi:10.1186/s12915-017-0390-6 (2017).
16. Schilling, C. et al. Sequence-Optimized Peptide Nanofibers as Growth Stimulators for Regeneration of Peripheral Neurons. *Advanced Functional Materials.* **1809112**, 1–15, doi:10.1002/adfm.201809112 (2019).
17. Chiki, A. et al. Mutant exon1 huntingtin aggregation is regulated by T3 phosphorylation-induced structural changes and crosstalk between T3 phosphorylation and acetylation at K6. *Angewandte Chemie - International Edition.* **56**, 5202–5207, doi:10.1002/anie.201611750 (2017).
18. Sieste, S. et al. Water-dispersible polydopamine-coated nanofibers for stimulation of neuronal growth and adhesion. *Advanced Healthcare Materials.* **7**, 1–11, doi:10.1002/adhm.201701485 (2018).
19. De, S. et al. Different soluble aggregates of Aβ42 can give rise to cellular toxicity through different mechanisms. *Nature Communications.* **10**, 1541, doi:10.1038/s41467-019-09477-3 (2019).
20. Chang, K. C., Chiang, Y. W., Yang, C. H., Liou, J. W. Atomic force microscopy in biology and biomedicine. *Tzu Chi Medical Journal.* **24**, 162–169, doi:10.1016/j.tcmj.2012.08.002 (2012).
21. Variola, F. Atomic force microscopy in biomaterials surface science. *Physical Chemistry Chemical Physics.* **17**, 2950–2959, doi:10.1039/c4cp04427d (2015).
22. Drolle, E., Hane, F., Lee, B., Leonenko, Z. Atomic force microscopy to study molecular mechanisms of amyloid fibril formation and toxicity in Alzheimer's disease. *Drug Metabolism Reviews.* **46**, 207–223, doi:10.3109/03602532.2014.882354 (2014).
23. Ruggeri, F. S. et al. Identification and nanomechanical characterization of the fundamental single-strand protofilaments of amyloid α-synuclein fibrils. *Proceedings of the National Academy of Sciences of the United States of America.* **115** (28), 7230–7235, doi:10.1073/PNAS.1721220115 (2018). doi:10.1073/PNAS.1721220115
24. Ruggeri, F. S. et al. Infrared nanospectroscopy characterization of oligomeric and fibrillar aggregates during amyloid formation. *Nature Communications.* **6**, 1–9, doi:10.1038/ncomms8831 (2015).

661 25. Ruggeri, F. S. et al. Microfluidic deposition for resolving single-molecule protein architecture
662 and heterogeneity. *Nature Communications.* **9**, doi:10.1038/s41467-018-06345-4 (2018).
663 26. Qamar, S. et al. FUS phase peparation is modulated by a molecular chaperone and
664 methylation of arginine cation-π interactions. *Cell.* **173**, 720-734.e15,
665 doi:10.1016/j.cell.2018.03.056 (2018).
666 27. Habchi, J. et al. Cholesterol catalyses Aβ42 aggregation through a heterogeneous nucleation
667 pathway in the presence of lipid membranes. *Nature Chemistry.* **10**, 673–683,
668 doi:10.1038/s41557-018-0031-x (2018).
669 28. Sweers, K. K. M., Stöckl, M., Bennink, M. L., Subramaniam, V. Characterizing nanoscale
670 morphologic and mechanical properties of α-Synuclein amyloid fibrils with atomic force
671 microscopy. In *Bio-nanoimaging: Protein Misfolding & Aggregation.* Edited by Uversky V. N.,
672 Lyubchenko, Y. L., 309–322, Elsevier. London, UK (2014).
673 29. Goldsbury, C. et al. Amyloid structure and assembly : Insights from scanning transmission
674 electron microscopy. *Journal of Structural Biology.* **173**, 1–13, doi:10.1016/j.jsb.2010.09.018
675 (2011).
676 30. Knowles, T. P. J., Smith, J. F., Devlin, G. L., Dobson, C. M., Welland, M. E. Analysis of structural
677 order in amyloid fibrils. *Nanotechnology.* **18**, doi:10.1088/0957-4484/18/4/044031 (2007).
678 31. Knowles, T. P. J., Mezzenga, R. Amyloid fibrils as building blocks for natural and artificial
679 functional materials. *Advanced Materials.* 6546–6561, doi:10.1002/adma.201505961 (2016).
680 32. Knowles, T. P. J., Oppenheim, T. W., Buell, A. K., Chirgadze, D. Y., Welland, M. E.
681 Nanostructured films from hierarchical self-assembly of amyloidogenic proteins. *Nature*
682 *Nanotechnology.* **5**, 204–207, doi:10.1038/nnano.2010.26 (2010).
683 33. Knowles, T. P. J., Smith, J. F., Craig, A., Dobson, C. M., Welland, M. E. Spatial persistence of
684 angular correlations in amyloid fibrils. *Physical Review Letters.* **96**, 1–4,
685 doi:10.1103/PhysRevLett.96.238301 (2006).
686 34. Knowles, T. P. J. et al. Twisting transition between crystalline and fibrillar phases of
687 aggregated peptides. *Physical Review Letters.* **109**, 158101,
688 doi:10.1103/PhysRevLett.109.158101 (2012).
689 35. Knowles, T. P. et al. Role of intermolecular forces in defining material properties of protein
690 nanofibrils. *Science.* **318**, 1900–1903, doi:10.1126/science.1150057 (2007).
691 36. Smith, J. F., Knowles, T. P. J., Dobson, C. M., MacPhee, C. E., Welland, M. E. Characterization
692 of the nanoscale properties of individual amyloid fibrils. *Proceedings of the National Academy of*
693 *Sciences of the United States of America.* **103**, 15806–15811, doi:10.1073/pnas.0604035103
694 (2006).
695 37. Sokolov, D. V. Atomic force microscopy for protein nanotechnology. *Methods in Molecular*
696 *Biology (Clifton, N.J.).* **300**, 323–367, doi:10.1007/978-1-62703-354-1_19 (2013).
697 38. Ruggeri, F. S. et al. Influence of the β-sheet content on the mechanical properties of
698 aggregates during amyloid fibrillization. *Angewandte Chemie - International Edition.* **54**, 2462–
699 2466, doi:10.1002/anie.201409050 (2015).
700 39. Jeong, J. S., Ansaloni, A., Mezzenga, R., Lashuel, H. A., Dietler, G. Novel mechanistic insight
701 into the molecular basis of amyloid polymorphism and secondary nucleation during amyloid
702 formation. *Journal of Molecular Biology.* **425**, 1765–1781, doi:10.1016/j.jmb.2013.02.005 (2013).
703 40. Adamcik, J., Mezzenga, R. Study of amyloid fibrils via atomic force microscopy. *Current*
704 *Opinion in Colloid and Interface Science.* **17**, 369–376, doi:10.1016/j.cocis.2012.08.001 (2012).

41. Deguire, S. M. et al. N-terminal huntingtin (Htt) phosphorylation is a molecular switch regulating Htt aggregation, helical conformation, internalization, and nuclear targeting. *Journal of Biological Chemistry.* jbc.RA118.004621, doi:10.1074/jbc.RA118.004621 (2018).
42. Ruggeri, F. S. et al. Nanoscale studies link amyloid maturity with polyglutamine diseases onset. *Scientific Reports.* **6**, 1–11, doi:10.1038/srep31155 (2016).
43. Adamcik, J. et al. Understanding amyloid aggregation by statistical analysis of atomic force microscopy images. *Nature Nanotechnology.* **5**, 423–428, doi:10.1038/nnano.2010.59 (2010).
44. Lin, Y. C., Komatsu, H., Ma, J., Axelsen, P. H., Fakhraai, Z. Quantitative analysis of amyloid polymorphism using height histograms to correct for tip convolution effects in atomic force microscopy imaging. *RSC Advances.* **6**, 114286–114295, doi:10.1039/C6RA24031C (2016).
45. Mannini, B. et al. Stabilization and characterization of cytotoxic Aβ40 oligomers isolated from an aggregation reaction in the presence of zinc ions. *ACS Chemical Neuroscience.* doi:10.1021/acschemneuro.8b00141 (2018).
46. Medalsy, I., Hensen, U., Muller, D. J. Imaging and quantifying chemical and physical properties of native proteins at molecular resolution by force-volume AFM. *Angewandte Chemie - International Edition.* **50**, 12103–12108, doi:10.1002/anie.201103991 (2011).
47. Dufrêne, Y. F., Martínez-Martín, D., Medalsy, I., Alsteens, D., Müller, D. J. Multiparametric imaging of biological systems by force-distance curve–based AFM. *Nature Methods.* **10**, 847–854, doi:10.1038/nmeth.2602 (2013).
48. Takai, E. et al. Scanning electron microscope imaging of amyloid fibrils. *American Journal of Biochemistry and Biotechnology.* **10**, 31–39, doi:10.3844/ajbbsp.2014.31.39 (2014).
49. Dazzi, A. et al. AFM-IR: Combining atomic force microscopy and infrared spectroscopy for nanoscale chemical characterization. *Applied Spectroscopy.* **66**, 1365–1384, doi:10.1366/12-06804 (2012).
50. Volpatti, L. R. et al. Micro- and nanoscale hierarchical structure of core-shell protein microgels. *Journal of Materials Chemistry B.* **4**, 7989–7999, doi:10.1039/c6tb02683d (2016).
51. Galante, D. et al. A critical concentration of N-terminal pyroglutamylated amyloid beta drives the misfolding of Ab1-42 into more toxic aggregates. *The International Journal of Biochemistry & Cell Biology.* **79**, 261–270, doi:10.1016/j.biocel.2016.08.037 (2016).
52. Ruggeri, F. S. et al. Identification of oxidative stress in red blood cells with nanoscale chemical resolution by infrared nanospectroscopy. *International Journal of Molecular Sciences.* **19**, 1–14, doi:10.3390/ijms19092582 (2018).
53. Ramer, G., Ruggeri, F. S., Levin, A., Knowles, T. P. J., Centrone, A. Determination of polypeptide conformation with nanoscale resolution in water. *ACS Nano*. **12** (7), 6612–6619, doi:10.1021/acsnano.8b01425 (2018).
54. Dazzi, A., Prater, C. B. AFM-IR: Technology and applications in nanoscale infrared spectroscopy and chemical imaging. *Chemical Reviews.* **117**, 5146–5173, doi:10.1021/acs.chemrev.6b00448 (2017).
55. Lahiri, B., Holland, G., Centrone, A. Chemical imaging beyond the diffraction limit: experimental validation of the PTIR technique. *Small.* **9** (3), 439–445, doi:10.1002/smll.201200788 (2013).
56. Ansaloni, A. et al. One-pot semisynthesis of exon 1 of the huntingtin protein: New tools for elucidating the role of posttranslational modifications in the pathogenesis of Huntington's disease. *Angewandte Chemie - International Edition.* **53** (7), 1928–1933,

doi:10.1002/anie.201307510 (2014).
57. Khalaf, O. et al. The H50Q mutation enhances α-synuclein aggregation, secretion, and toxicity. *Journal of Biological Chemistry.* **289**, 21856–21876, doi:10.1074/jbc.M114.553297 (2014).
58. Hellstrand, E., Boland, B., Walsh, D. M., Linse, S. Amyloid β-protein aggregation produces highly reproducible kinetic data and occurs by a two-phase process. *ACS Chemical Neuroscience.* **1**, 13–18, doi:10.1021/cn900015v (2010).
59. Limbocker, R. et al. Trodusquemine enhances Aβ42 aggregation but suppresses its toxicity by displacing oligomers from cell membranes. *Nature Communications.* **10** (1), 225, doi:10.1038/s41467-018-07699-5 (2019).
60. Lu, F., Belkin, M. A. Infrared absorption nano-spectroscopy using sample photoexpansion induced by tunable quantum cascade lasers. *Optics Express.* **19**, 1902–1904 (2011).
61. Jiao, Y., Schäffer, T. E. Accurate height and volume measurements on soft samples with the atomic force microscope. *Langmuir.* **20**, 10038–10045, doi:10.1021/la048650u (2004).
62. Müller, D. J., Engel, A. The height of biomolecules measured with the atomic force microscope depends on electrostatic interactions. *Biophysical Journal.* **73**, 1633–1644, doi:10.1016/S0006-3495(97)78195-5 (1997).
63. Heymann, J. B., Moller, C., Muller, D. J. Sampling effects influence heights measured with atomic force microscopy. *Journal Of Microscopy-Oxford.* **207**, 43–51, doi:10.1111/j.1365-2818.2007.01837.x (2002).
64. Marinello, F., Balcon, M., Schiavuta, P., Carmignato, S., Savio, E. Thermal drift study on different commercial scanning probe microscopes during the initial warming-up phase. *Measurement Science and Technology.* **22**, 9, doi:10.1088/0957-0233/22/9/094016 (2011).
65. Marinello, F., Bariani, P., De Chiffre, L., Savio, E. Fast technique for AFM vertical drift compensation. *Measurement Science and Technology.* **18**, 689–696, doi:10.1088/0957-0233/18/3/019 (2007).
66. Ricci, D., Braga, P. C. Recognizing and avoiding artifacts in AFM imaging. *Methods in Molecular Biology (Clifton, N.J.).* **242**, 25–37, doi:10.1385/1-59259-647-9:25 (2004).
67. Canale, C., Torre, B., Ricci, D., Braga, P. C. Recognizing and avoiding artifacts in atomic force microscopy imaging. In *Atomic Force Microscopy in Biomedical Research.* Edited by Braga, P. C., Ricci, D., **736**, 31–43, Humana Press. New York, NY (2011).
68. Marinello, F., Carmignato, S., Voltan, A., Savio, E., De Chiffre, L. Error Sources in Atomic Force Microscopy for Dimensional Measurements: Taxonomy and Modeling. *Journal of Manufacturing Science and Engineering.* **132**, 030903, doi:10.1115/1.4001242 (2010).
69. Ukraintsev, E., Kromka, A., Kozak, H., Reme, Z., Rezek, B. Artifacts in Atomic Force Microscopy of Biological Samples. In *Atomic Force Microscopy Investigations into Biology - From Cell to Protein.* Edited by Frewin, C. L., doi:10.5772/36203, InTechOpen. (2012).
70. Tsukruk, V. V., Singamaneni, S. *Scanning Probe Microscopy of Soft Matter: Fundamentals and Practices*. Wiley-VCH Verlag GmbH & Co. KGaA. Weinheim, Germany (2011).

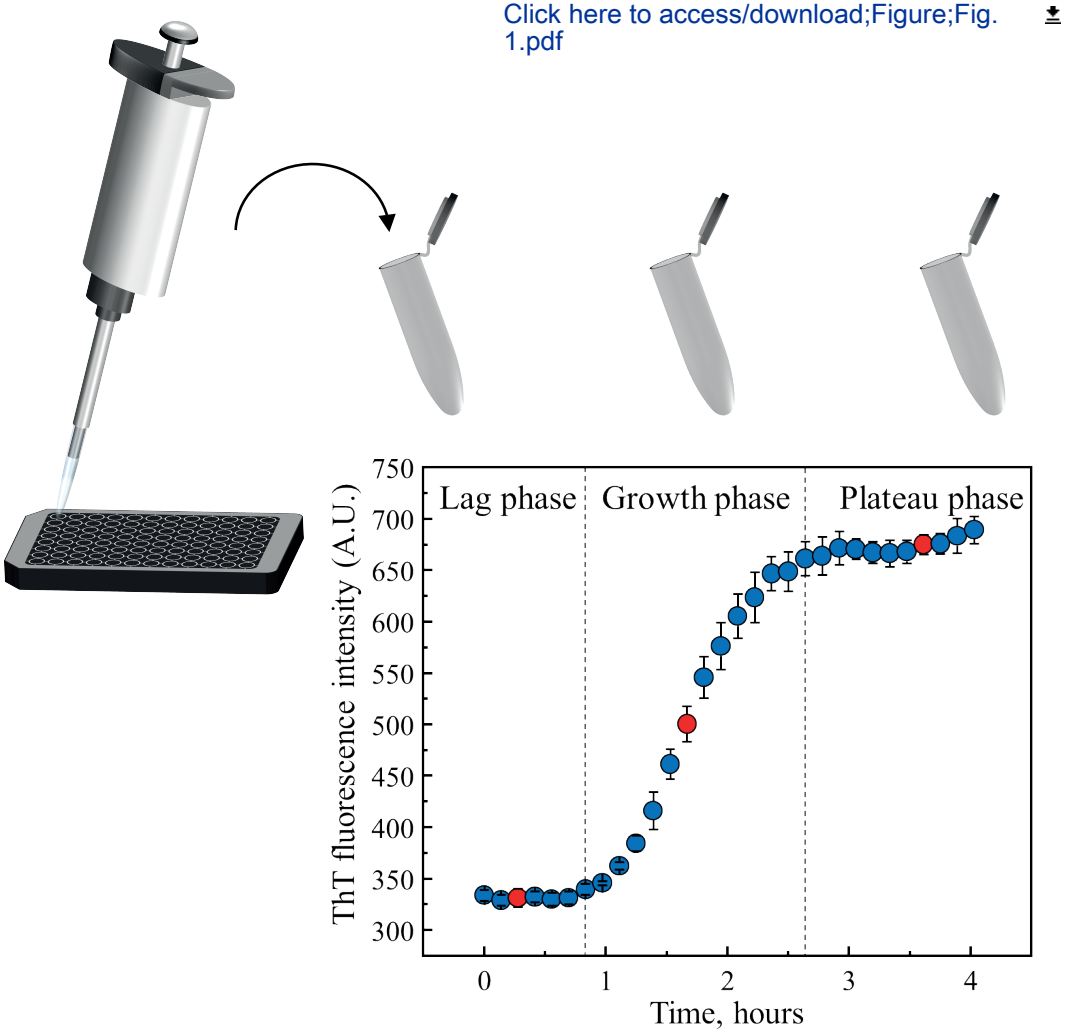

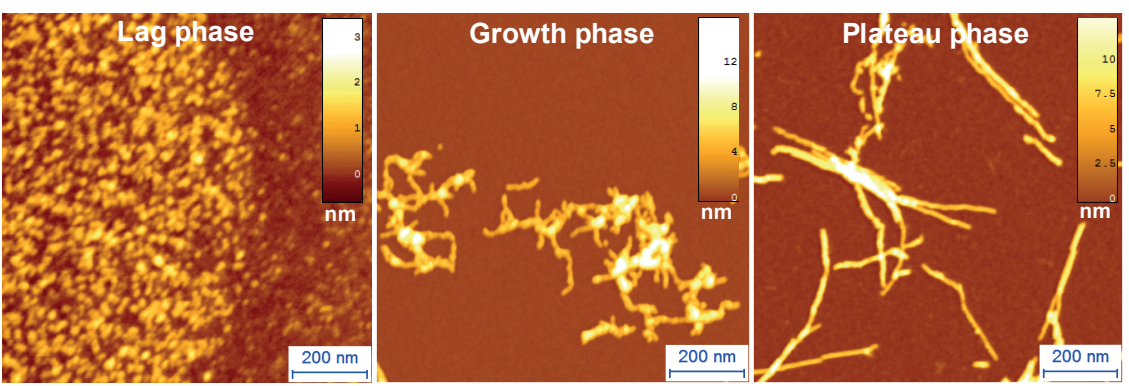

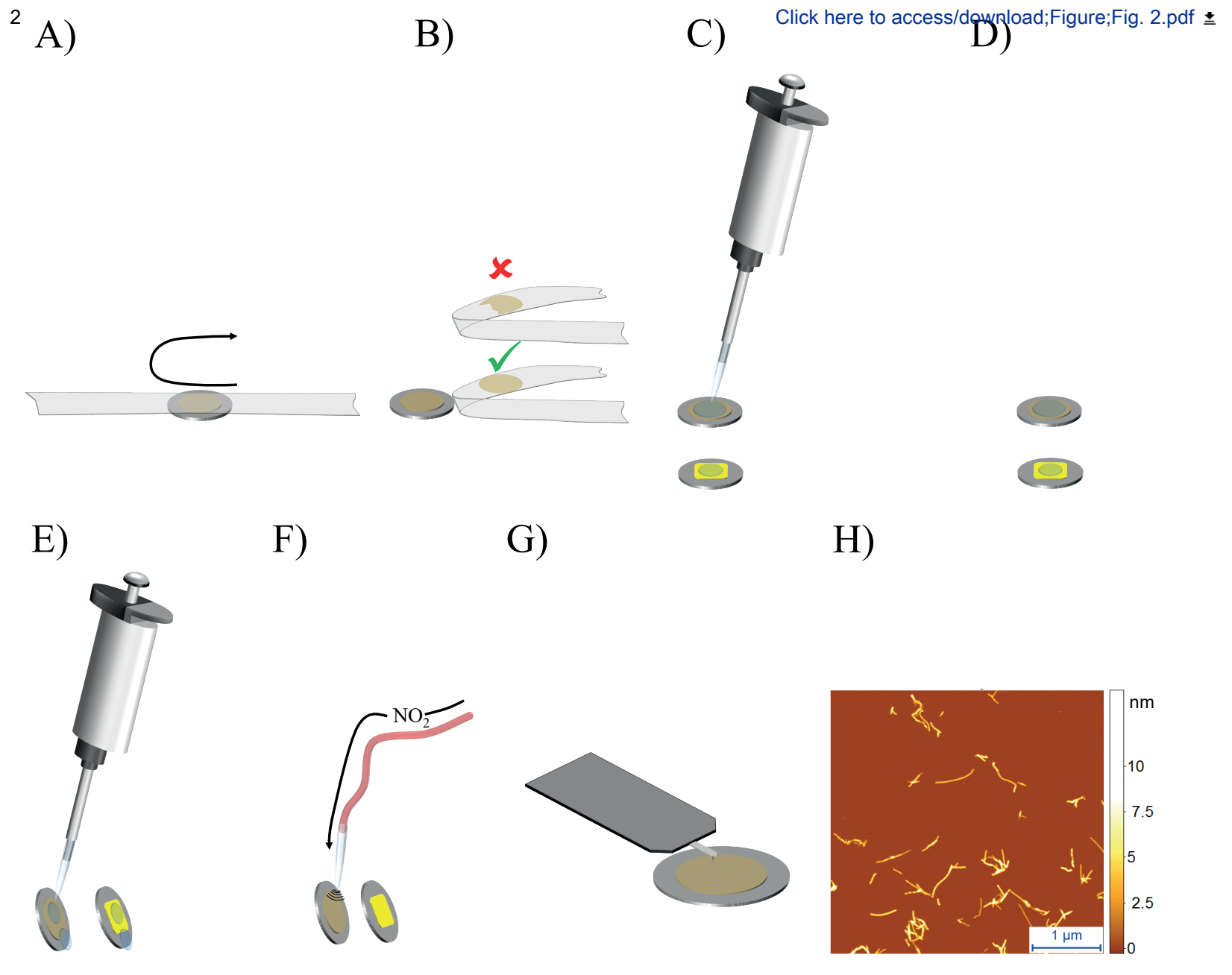

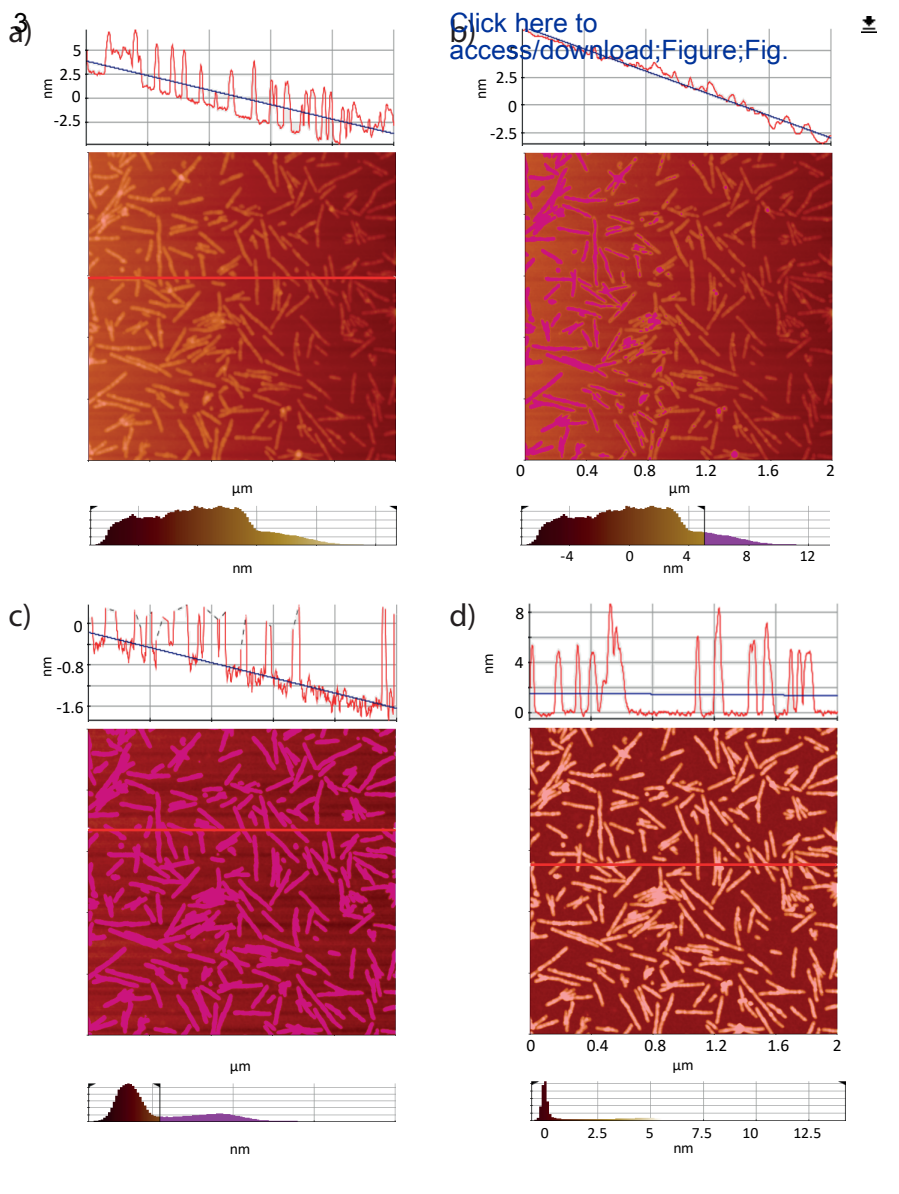

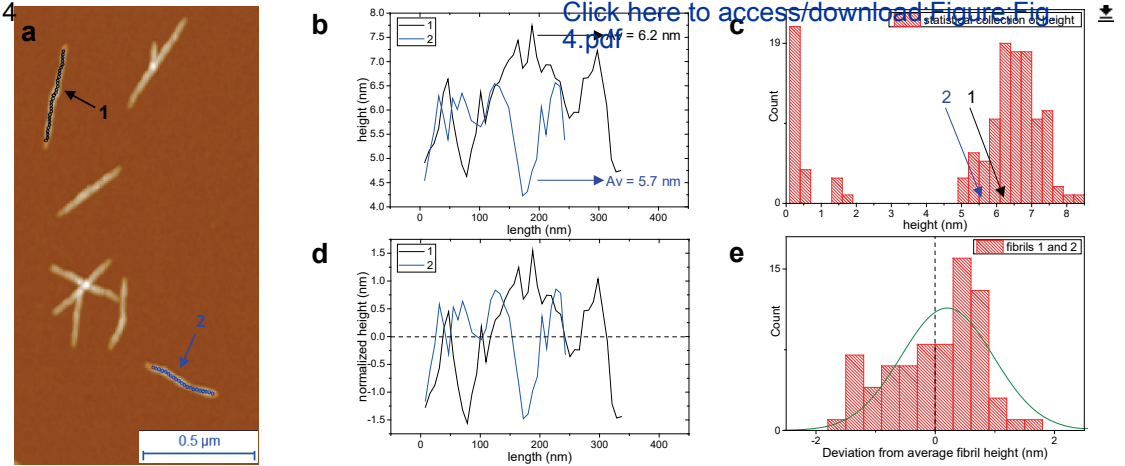

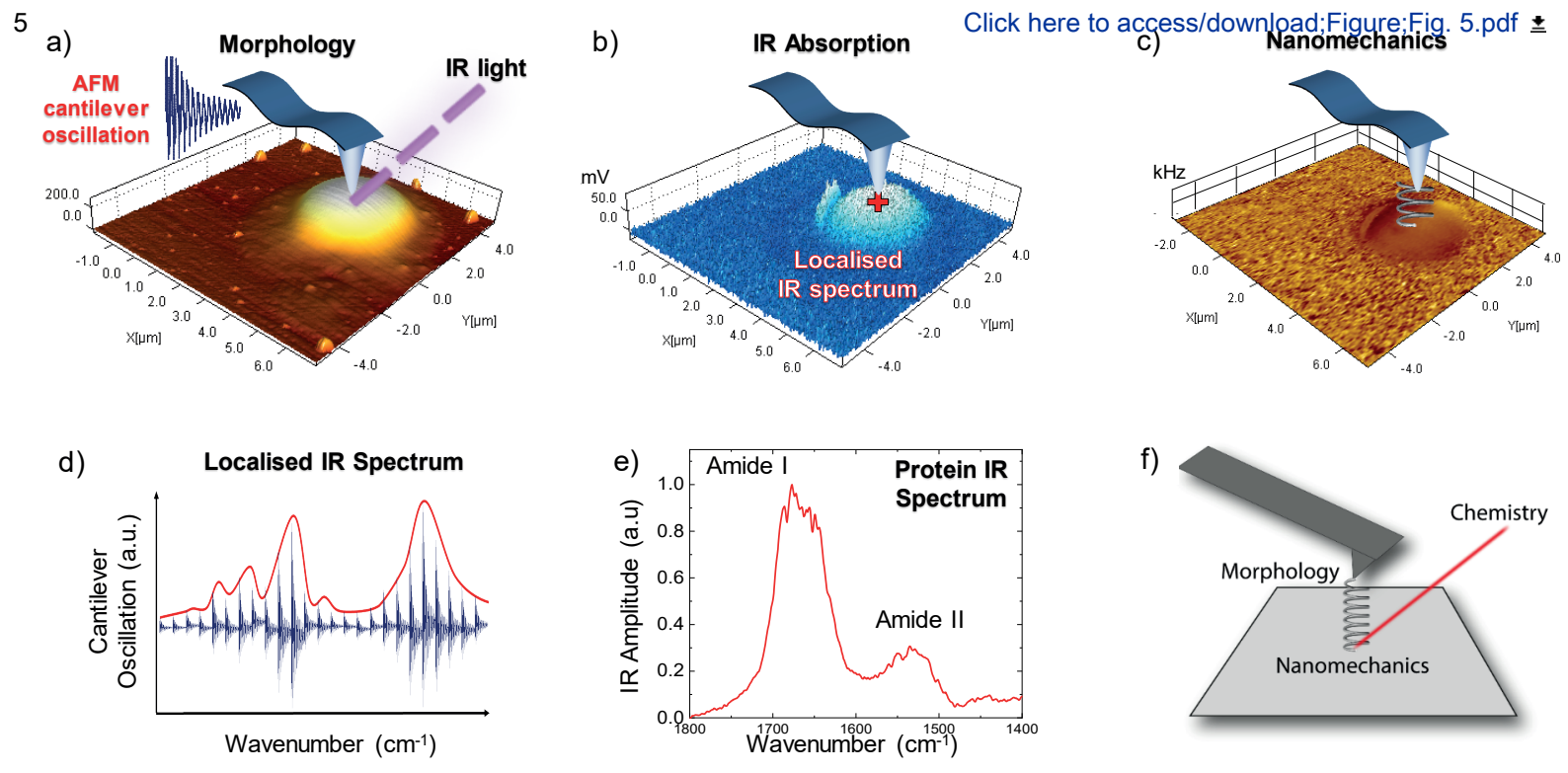

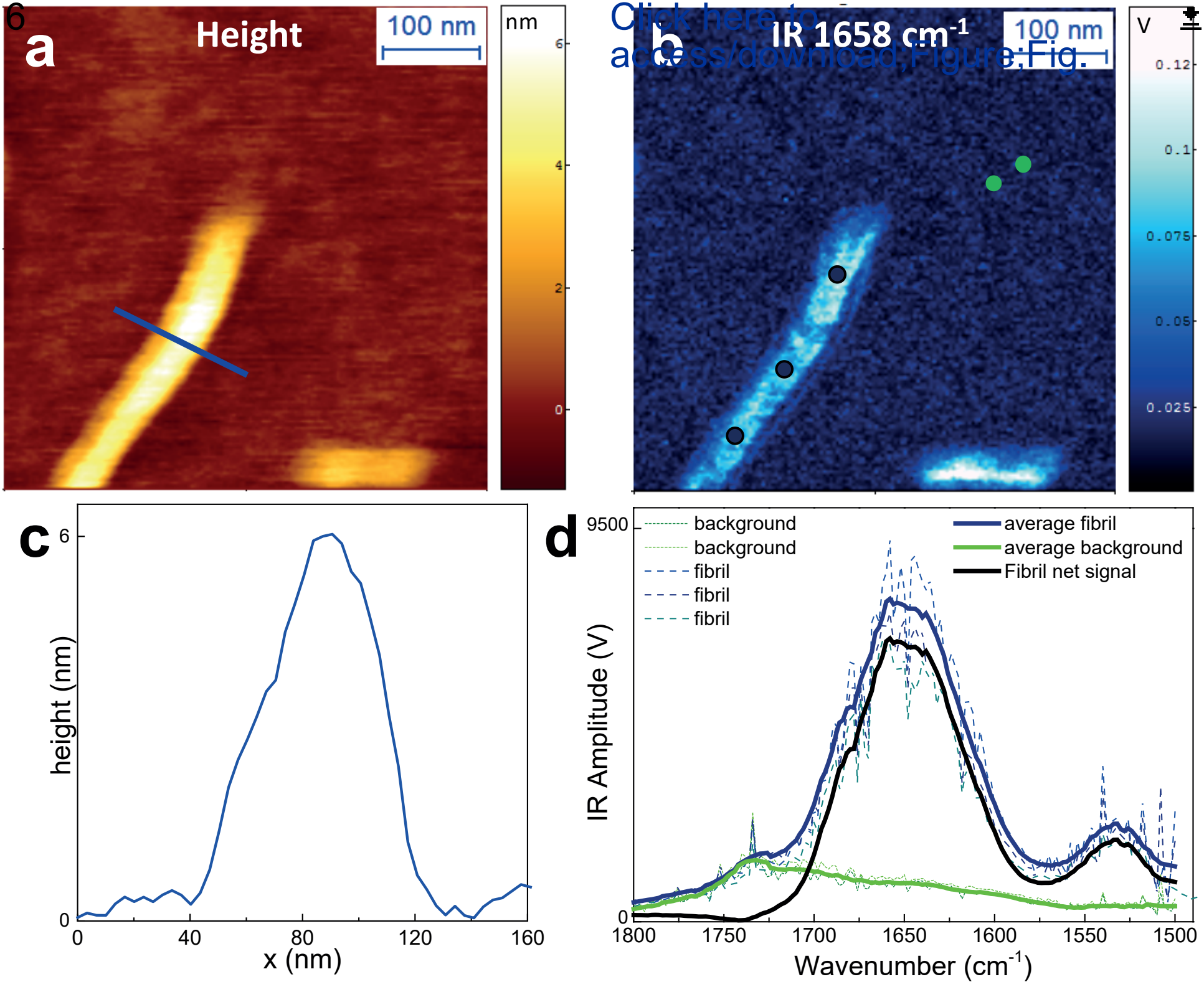

Table of Materials

Click here to access/download;Table of Materials;60108_Materials.xlsx

Name of Material/ Equipment	Company	Catalog Number
AFM-IR system	Anasys Instruments	nanoIR 2 or 3
Corning 96-well Half Area Black/Clear Bottom Polystyrene NBS Microplate	Corning	3881
Corning Microplate Aluminium Sealing Tape	Corning	6570
Double Sided Adhesive Discs	AGAR Scientific	AGG3347N
FLUOstar Omega	BMG Labtech	415-101
Mica Disc 10mm V1	AGAR Scientific	AGF7013
Park NX10 AFM system	Park Systems	N/A
Platypus Ultra-Flat Gold Chips	Platypus Technologies	AU.1000.SWTSG
PPP-NCHR-10 cantilevers	Park Systems	PPP-NCHR-10
Protein LowBind Tubes, 2.0mL	Eppendorf	30108132
Silicon gold coated cantilevers	Anasys Instruments	PR-EX-nIR2
SPM Specimen Discs 12mm	AGAR Scientific	AGF7001

Comments/Description

Systems to measure thermal expansion in contact and resonance mode

Platereader

Atomic Force Microscope

jove JOURNAL OF VISUALIZED EXPERIMENTS
1 Alewife Center #200
Cambridge, MA 02140
tel. 617.945.9051
www.jove.com

ARTICLE AND VIDEO LICENSE AGREEMENT - UK

Title of Article:	Characterising Individual Amyloid Aggregates by Infrared Nanospectroscopy and Atomic Force Microscopy
Author(s):	Francesco Simone Ruggeri*, Tomas Šneideris, Sean Chia, Michele Vendruscolo, Tuomas P. J. Knowles*

Item 1: The Author elects to have the Materials be made available (as described at http://www.jove.com/publish) via:

☒ Standard Access ☐ Open Access

Item 2: Please select one of the following items:

☒ The Author is **NOT** a United States government employee.

☐ The Author is a United States government employee and the Materials were prepared in the course of his or her duties as a United States government employee.

☐ The Author is a United States government employee but the Materials were NOT prepared in the course of his or her duties as a United States government employee.

ARTICLE AND VIDEO LICENSE AGREEMENT

1. **Defined Terms.** As used in this Article and Video License Agreement, the following terms shall have the following meanings: "**Agreement**" means this Article and Video License Agreement; "**Article**" means the article specified on the last page of this Agreement, including any associated materials such as texts, figures, tables, artwork, abstracts, or summaries contained therein; "**Author**" means the author who is a signatory to this Agreement; "**Collective Work**" means a work, such as a periodical issue, anthology or encyclopedia, in which the Materials in their entirety in unmodified form, along with a number of other contributions, constituting separate and independent works in themselves, are assembled into a collective whole; "**CRC License**" means the Creative Commons Attribution 3.0 Agreement (also known as CC-BY), the terms and conditions of which can be found at: http://creativecommons.org/licenses/by/3.0/us/legalcode ; "**Derivative Work**" means a work based upon the Materials or upon the Materials and other pre-existing works, such as a translation, musical arrangement, dramatization, fictionalization, motion picture version, sound recording, art reproduction, abridgment, condensation, or any other form in which the Materials may be recast, transformed, or adapted; "**Institution**" means the institution, listed on the last page of this Agreement, by which the Author was employed at the time of the creation of the Materials; "**JoVE**" means MyJove Corporation, a Massachusetts corporation and the publisher of The Journal of Visualized Experiments; "**Materials**" means the Article and / or the Video; "**Parties**" means the Author and JoVE; "**Video**" means any video(s) made by the Author, alone or in conjunction with any other parties, or by JoVE or its affiliates or agents, individually or in collaboration with the Author or any other parties, incorporating all or any portion of the Article, and in which the Author may or may not appear.

2. **Background.** The Author, who is the author of the Article, in order to ensure the dissemination and protection of the Article, desires to have the JoVE publish the Article and create and transmit videos based on the Article. In furtherance of such goals, the Parties desire to memorialize in this Agreement the respective rights of each Party in and to the Article and the Video.

3. **Grant of Rights in Article.** In consideration of JoVE agreeing to publish the Article, the Author hereby grants to JoVE, subject to **Sections 4 and 7** below, the exclusive, royalty-free, perpetual (for the full term of copyright in the Article, including any extensions thereto) license (a) to publish, reproduce, distribute, display and store the Article in all forms, formats and media whether now known or hereafter developed (including without limitation in print, digital and electronic form) throughout the world, (b) to translate the Article into other languages, create adaptations, summaries or extracts of the Article or other Derivative Works (including, without limitation, the Video) or Collective Works based on all or any portion of the Article and exercise all of the rights set forth in (a) above in such translations, adaptations, summaries, extracts, Derivative Works or Collective Works and (c) to license others to do any or all of the above. The foregoing rights may be exercised in all media and formats, whether now known or hereafter devised, and include the right to make such modifications as are technically necessary to exercise the rights in other media and formats. If the "Open Access" box has been checked in **Item 1** above, JoVE and the Author hereby grant to the public all such rights in the Article as provided in, but subject to all limitations and requirements set forth in, the CRC License.

4. **Retention of Rights in Article.** Notwithstanding the exclusive license granted to JoVE in **Section 3** above, the Author shall, with respect to the Article, retain the non-exclusive right to use all or part of the Article for the non-commercial purpose of giving lectures, presentations or teaching classes, and to post a copy of the Article on the Institution's website or the Author's personal website, in each case provided that a link to the Article on the JoVE website is provided and notice of JoVE's copyright in the Article is included. All non-copyright intellectual property rights in and to the Article, such as patent rights, shall remain with the Author.

5. **Grant of Rights in Video - Standard Access.** This **Section 5** applies if the "Standard Access" box has been checked in **Item 1** above or if no box has been checked in **Item 1** above. In consideration of JoVE agreeing to produce, display or otherwise assist with the Video, the Author hereby acknowledges and agrees that, subject to **Section 7** below, JoVE is and shall be the sole and exclusive owner of all rights of any nature, including, without limitation, all copyrights, in and to the Video. To the extent that, by law, the Author is deemed, now or at any time in the future, to have any rights of any nature in or to the Video, the Author hereby disclaims all such rights and transfers all such rights to JoVE.

6. **Grant of Rights in Video - Open Access.** This **Section 6** applies only if the "Open Access" box has been checked in **Item 1** above. In consideration of JoVE agreeing to produce, display or otherwise assist with the Video, the Author hereby grants to JoVE, subject to **Section 7** below, the exclusive, royalty-free, perpetual (for the full term of copyright in the Article, including any extensions thereto) license (a) to publish, reproduce, distribute, display and store the Video in all forms, formats and media whether now known or hereafter developed (including without limitation in print, digital and electronic form) throughout the world, (b) to translate the Video into other languages, create adaptations, summaries or extracts of the Video or other Derivative Works or Collective Works based on all or any portion of the Video and exercise all of the rights set forth in (a) above in such translations, adaptations, summaries, extracts, Derivative Works or Collective Works and (c) to license others to do any or all of the above. The foregoing rights may be exercised in all media and formats, whether now known or hereafter devised, and include the right to make such modifications as are technically necessary to exercise the rights in other media and formats.

7. **Government Employees.** If the Author is a United States government employee and the Article was prepared in the course of his or her duties as a United States government employee, as indicated in **Item 2** above, and any of the licenses or grants granted by the Author hereunder exceed the scope of the 17 U.S.C. 403, then the rights granted hereunder shall be limited to the maximum rights permitted under such statute. In such case, all provisions contained herein that are not in conflict with such statute shall remain in full force and effect, and all provisions contained herein that do so conflict shall be deemed to be amended so as to provide to JoVE the maximum rights permissible within such statute.

8. **Protection of the work.** The Author(s) authorize JoVE to take steps in the Author(s) name and on their behalf if JoVE believes some third party could be infringing or might infringe the copyright of either the Author's Article and/or Video.

9. **Likeness, Privacy, Personality.** The Author hereby grants JoVE the right to use the Author's name, voice, likeness, picture, photograph, image, biography and performance in any way, commercial or otherwise, in connection with the Materials and the sale, promotion and distribution thereof. The Author hereby waives any and all rights he or she may have, relating to his or her appearance in the Video or otherwise relating to the Materials, under all applicable privacy, likeness, personality or similar laws.

10. **Author Warranties**. The Author represents and warrants that the Article is original, that it has not been published, that the copyright interest is owned by the Author (or, if more than one author is listed at the beginning of this Agreement, by such authors collectively) and has not been assigned, licensed, or otherwise transferred to any other party. The Author represents and warrants that the author(s) listed at the top of this Agreement are the only authors of the Materials. If more than one author is listed at the top of this Agreement and if any such author has not entered into a separate Article and Video License Agreement with JoVE relating to the Materials, the Author represents and warrants that the Author has been authorized by each of the other such authors to execute this Agreement on his or her behalf and to bind him or her with respect to the terms of this Agreement as if each of them had been a party hereto as an Author. The Author warrants that the use, reproduction, distribution, public or private performance or display, and/or modification of all or any portion of the Materials does not and will not violate, infringe and/or misappropriate the patent, trademark, intellectual property or other rights of any third party. The Author represents and warrants that it has and will continue to comply with all government, institutional and other regulations, including, without limitation all institutional, laboratory, hospital, ethical, human and animal treatment, privacy, and all other rules, regulations, laws, procedures or guidelines, applicable to the Materials, and that all research involving human and animal subjects has been approved by the Author's relevant institutional review board.

11. **JoVE Discretion.** If the Author requests the assistance of JoVE in producing the Video in the Author's facility, the Author shall ensure that the presence of JoVE employees, agents or independent contractors is in accordance with the relevant regulations of the Author's institution. If more than one author is listed at the beginning of this Agreement, JoVE may, in its sole discretion, elect not take any action with respect to the Article until such time as it has received complete, executed Article and Video License Agreements from each such author. JoVE reserves the right, in its absolute and sole

jove JOURNAL OF VISUALIZED EXPERIMENTS
1 Alewife Center #200
Cambridge, MA 02140
tel. 617.945.9051
www.jove.com

ARTICLE AND VIDEO LICENSE AGREEMENT - UK

discretion andwithout giving any reason therefore, to accept or decline any work submitted to JoVE. JoVE and its employees, agents and independent contractors shall have full, unfettered access to the facilities of the Author or of the Author's institution as necessary to make the Video, whether actually published or not. JoVE has sole discretion as to the method of making and publishing the Materials, including, without limitation, to all decisions regarding editing, lighting, filming, timing of publication, if any, length, quality, content and the like.

12. **Indemnification.** The Author agrees to indemnify JoVE and/or its successors and assigns from and against any and all claims, costs, and expenses, including attorney's fees, arising out of any breach of any warranty or other representations contained herein. The Author further agrees to indemnify and hold harmless JoVE from and against any and all claims, costs, and expenses, including attorney's fees, resulting from the breach by the Author of any representation or warranty contained herein or from allegations or instances of violation of intellectual property rights, damage to the Author's or the Author's institution's facilities, fraud, libel, defamation, research, equipment, experiments, property damage, personal injury, violations of institutional, laboratory, hospital, ethical, human and animal treatment, privacy or other rules, regulations, laws, procedures or guidelines, liabilities and other losses or damages related in any way to the submission of work to JoVE, making of videos by JoVE, or publication in JoVE or elsewhere by JoVE. The Author shall be responsible for, and shall hold JoVE harmless from, damages caused by lack of sterilization, lack of cleanliness or by contaminationdue to the making of a video by JoVE its employees, agents or independent contractors. All sterilization, cleanliness or decontamination procedures shall be solely the responsibility of the Author and shall be undertaken at the Author's expense. All indemnifications provided herein shall include JoVE's attorney's fees and costs related to said losses or damages. Such indemnification and holding harmless shall include such losses or damages incurred by, or in connection with, acts or omissions of JoVE, its employees, agents or independent contractors.

13. **Fees.** To cover the cost incurred for publication, Jo VE must receive payment before production and publication the Materials. Payment is due in 21 days of invoice. Should the Materials not be published due to an editorial or production decision, these funds will be returned to the Author. Withdrawal by the Author of any submitted Materials after final peer review approval will result in a US$1,200 fee to cover pre-production expenses incurred by JoVE. If payment is not received by the completion of filming, production and publication of the Materials will be suspended until payment is received.

14. **Transfer, Governing Law.** This Agreement may be assigned by JoVE and shall inure to the benefits of any of JoVE's successors and assignees. This Agreement shall be governed and construed by the internal laws of the Commonwealth of Massachusetts without giving effect to any conflict of law provision thereunder. This Agreement may be executed in counterparts, each of which shall be deemed an original, but all of which together shall be deemed to me one and the same agreement. A signed copy of this Agreement delivered by facsimile, e-mail or other means of electronic transmission shall be deemed to have the same legal effect as delivery of an original signed copy of this Agreement.

A signed copy of this document must be sent with all new submissions. Only one Agreement is required per submission.

CORRESPONDING AUTHOR

Name:	Francesco Simone Ruggeri
Department:	Department of Chemistry
Institution:	University of Cambridge
Title:	Research Fellow
Signature:	
Date:	28/04/2019

Please submit a **signed** and **dated** copy of this license by one of the following three methods:

1. Upload an electronic version on the JoVE submission site
2. Fax the document to +1.866.381.2236
3. Mail the document to JoVE / Attn: JoVE Editorial / 1 Alewife Center #200 / Cambridge, MA 02140

Centre for Misfolding Disease
Department of Chemistry
CB2 1EW, Cambridge
United Kingdom

Corresponding Author: Dr. Francesco Simone Ruggeri
Telephone : +44 1223 336300
E-mail: fsr26@cam.ac.uk
Site web : http://www.cmd.ch.cam.ac.uk/

Dear Editor,

We should like to resubmit for consideration in your journal as article our manuscript *"Characterizing Individual Amyloid Aggregates by Infrared Nanospectroscopy and Atomic Force Microscopy*".

We are glad of the very positive response of the reviewers that recognized the value of the protocol. Their suggestions together with the editorial comments have greatly improved the manuscript.

We hope that now the manuscript is suitable for publication in Jove.

On behalf of all the authors,

F.S. Ruggeri and T. P. J. Knowles

Editorial Comments:

• Please take this opportunity to thoroughly proofread the manuscript to ensure that there are no spelling or grammatical errors.

• **Textual Overlap:** Significant portions show significant overlap with previously published work. Please re-write the text in lines 23-25, 38-60, 67-71, 79-89, 276-290, 395-400 to avoid this overlap.

Answer: We have rewritten the parts highlighted by the editor.

• **Protocol Detail:** Please note that your protocol will be used to generate the script for the video, and must contain everything that you would like shown in the video. **Please add more specific details (e.g. button clicks for software actions, numerical values for settings, etc) to your protocol steps.** There should be enough detail in each step to supplement the actions seen in the video so that viewers can easily replicate the protocol. Examples:

1) Section 5: all software actions must be described using explicit button clicks.

Answer: We have updated the protocol section.

• **Protocol Numbering:** Please adjust the numbering of your protocol section to follow JoVE's instructions for authors, 1. should be followed by 1.1. and then 1.1.1. if necessary and all steps should be lined up at the left margin with no indentations. There must also be a one-line space between each protocol step.

Answer: We have adjusted the numbering of the protocol.

• **Protocol Highlight:** After you have made all of the recommended changes to your protocol (listed above), please re-evaluate the length of your protocol section. There is a 10-page limit for the protocol text, and a 3- page limit for filmable content. If your protocol is longer than 3 pages, please highlight ~2.5 pages or less of text (which includes headings and spaces) in yellow, to identify which steps should be visualized to tell the most cohesive story of your protocol steps.

1) The highlighting must include all relevant details that are required to perform the step. For example, if step 2.5 is highlighted for filming and the details of how to perform the step are given in steps 2.5.1 and 2.5.2, then the sub-steps where the details are provided must be included in the highlighting.

2) The highlighted steps should form a cohesive narrative, that is, there must be a logical flow from one highlighted step to the next.

3) Please highlight complete sentences (not parts of sentences). Include sub-headings and spaces when calculating the final highlighted length.

4) Notes cannot be filmed and should be excluded from highlighting.

5) Please bear in mind that software steps without a graphical user interface/calculations/ command line scripting cannot be filmed.

Answer: We have highlighted the relevant parts.

• **Discussion:** JoVE articles are focused on the methods and the protocol, thus the discussion should be similarly focused. Please ensure that the discussion covers the following in detail and in paragraph form (3-6 paragraphs): 1) modifications and troubleshooting, 2) limitations of the technique, 3) significance with respect to existing methods, 4) future applications and 5) critical steps within the protocol.

Answer: We have updated the discussion.

• **References:**

1) Please move the in-text http weblinks (lines 109-110, 115, 123, 127, etc) into the reference list, and use superscripted citations. For product pages, please list all products in the table of materials instead.

2) Please spell out journal names.

Answer: Done.

• **Commercial Language:** JoVE is unable to publish manuscripts containing commercial sounding language, including trademark or registered trademark symbols (TM/R) and the mention of company brand names before an instrument or reagent. Examples of commercial sounding language in your manuscript are Eppendorf, Corning 3881, FLUOstar® plate readers from BMG Labtech, SPIP (Image Metrology), Bruker, PR-EX-nIR2, Bruker,

1) Please use MS Word's find function (Ctrl+F), to locate and replace all commercial sounding language in your manuscript with generic names that are not company-specific. All commercial products should be sufficiently referenced in the table of materials/reagents. You may use the generic term followed by "(see table of materials)" to draw the readers' attention to specific commercial names.

Answer: We have removed all commercial language and wording.

• If your figures and tables are original and not published previously or you have already obtained figure permissions, please ignore this comment. If you are re-using figures from a previous publication, you must obtain explicit permission to re-use the figure from the previous publisher (this can be in the form of a letter from an editor or a link to the editorial policies that allows you to re-publish the figure). Please upload the text of the re-print permission (may be copied and pasted from an email/website) as a Word document to the Editorial Manager site in the "Supplemental files (as requested by JoVE)" section. Please also cite the figure appropriately in the figure legend, i.e. "This figure has been modified from [citation]."

Answer: We have obtained explicit permissions to re-use the figures from ~~previous publishers.~~"Influence of the β-Sheet Content on the Mechanical Properties of Aggregates during Amyloid Fibrillization". The figures re-used from "Nanoscale studies link amyloid maturity with polyglutamine diseases onset" are licensed under a Creative Commons Attribution 4.0 International License. To view a copy of this license, please, visit http://creativecommons.org/licenses/by/4.0/

Formatted: English (United States), Pattern: Clear (White)

Comments from Peer-Reviewers:

Reviewer #1:

Manuscript Summary:

The paper submitted by author tries to use Infrared Nanospectroscopy (AFM-IR), simultaneously exploiting the high resolution of AFM and the chemical recognition power of infrared (IR) spectroscopy, as a versatile tool to characterize at the nanoscale the conformational rearrangements of proteins during their aggregation at the single molecule scale to understand how they misfold and aggregate. The author combined two conventional technologies Atomic Force Microscopy (AFM) and infrared (IR) spectroscopy to exploit the high resolution of AFM and the chemical recognition power of IR both. Introduction part is strong and satisfies the expectations and it does contain the information we need to find under the title. The title is clearly understandable and no inconsistency exists between the title and the content. Overall, the paper is comprehensive in terms of explaining the methodology. The general study and observations were accomplished in a comprehensive manner and the results are interesting. However, some minor clarifications required as to the details of the observations.

Answer: We would like to thank the reviewer for the very positive evaluation of the manuscript.

Major Concerns:
Clarifications required:

1. Abstract mentions about "Central importance in order to develop new pharmacological approach to neurodegenerative disorders." But no such recommendations or suggestions were made in the text itself.

Answer: We thank the reviewer for the suggestion, we have update the abstract and the discussion.

2. Selection criteria of Aβ42 peptide for this study in not clearly mentioned in text.

Answer: We have explained now in the text that we used the aggregation of Aβ42 peptide since it is involved in the onset of Alzheimer's disease and since it can be considered a model system to implement the protocol to study protein aggregation.

Minor Concerns:

1. The paper needs a careful proof-reading as there are some typos errors. Example: Line 348 contains "Tough powerful" which, in context seems to be inappropriate.

Answer: Corrected.

Reviewer #2:

The manuscript entitled characterising individual Amyloid aggregates by infrared Nanospectroscopy and Atomic force microscopy describe the procedure to determine the oligomerization process of AB42 which can be applied to several peptides or proteins employing AFM-IR.

Minor Concerns:

The same sample is processed in the same equipment, To obtain the information from AFM and IR.
How the AFM-IR help to know the oligomerization process.

Answer: The AFM-IR technique measures simultaneously the morphology and chemical properties. However, the aggregation process is performed *in vitro* and aliquots at different time points are deposited on the substrate to retrieve a picture of the process, included the early oligomerisation. For instance, the reviewer could refer to *Ruggeri, PNAS, 2018*.

Is clear that AFM identify the morphology, but is not clear if, IR identify the inter-chain interaction.

Answer: IR spectroscopy is sensitive to intermolecular hydrogen bonding occurring between proteins and thus to inter-chain interactions.

Also, could be important mention if the procedure is useful with other AFM equipment and also if the material that is necessary exist in different brands.

Answer: Originally, AFM-IR spectroscopy working through thermomechanical detection has been developed by “Anasys Instruments”, now purchased by “Bruker”. Recently, another company has developed an AFM-IR system, however it can measure only in non-contact mode, while in our work we necessitate of measuring in contact to have enough sensitivity.

The ThT assay depends on the peptide concentration and also how the assay is done, for example if the assay is done in a plate or in a cuvette, then these considerations could be mentioned, and how the author established the condition to do a kinetic correlation between ThT and AFM.

Answer: We agree with the reviewer that the kinetics assays are extremely sensitive. It is specified in the protocol that the aggregation assay is performed in a plate reader. We have added the relevant references in the text regarding how the protocol has been developed. For instance, the reviewer could refer to Hellstrand, ACS Chemical Neuroscience, 2009.

We did not establish any specific condition to correlate kinetics and AFM. At each specific time point of interest, an aliquot of the solution in the plate reader is deposited on a mica substrate for AFM analysis. The experiment is performed in triplicates.

Reviewer #3:

Manuscript Summary:

This MS describes protocol for imaging amyloid beta fibrils by multiple methods, presenting an opportunity to examine the mechanism of fibril self assembly. The protocol is highly detailed and useful.

Answer: We would like to thank the reviewer for the very positive evaluation of the protocol.

Major Concerns:

The article makes many claims of single molecule (monomer) sensitivity. This is not appropriate and reflects a misunderstanding of the infrared imaging technique. While the isolated monomers illustrate in Figure 1 can be monomers, the infrared signal from a beta fragments in the fibrils does not come from single a-beta monomers. There are simple ways to understand this. First, the spatial resolution of the instrument is not sharp enough to isolate a single AB42 peptide within the fibril. Second, the coupling of the IR resonances between sheets precludes the identification of the response as being from a single AB42 peptide (single molecule). There are intersheet couplings in the IR signal. The text needs to be edited to remove the claim of single molecule or monomer sensitivity. The claim is misleading.

Answer: We fully agree with the reviewer. While as in Fig. 1, AFM is capable to easily visualise an individual monomer (Ruggeri, PNAS, 2018; Ruggeri, Angewandte, 2015; Khalaf, JBC, 2015). AFM-IR has still limited chemical resolution. The smallest objects from which chemical information could be retrieved till now are lipid membrane monolayers or oligomeric amyloid aggregates with a radius of about 5 nm. We have now clarified this difference trough the text.

In other respects, the protocol would be of general interest and potentially useful.

Answer: We would like to thank the reviewer for the very positive evaluation of the manuscript.

JOHN WILEY AND SONS LICENSE TERMS AND CONDITIONS

Jun 02, 2019

This Agreement between University of Cambridge -- Tomas Sneideris ("You") and John Wiley and Sons ("John Wiley and Sons") consists of your license details and the terms and conditions provided by John Wiley and Sons and Copyright Clearance Center.

License Number	4600760921419
License date	Jun 02, 2019
Licensed Content Publisher	John Wiley and Sons
Licensed Content Publication	Angewandte Chemie International Edition
Licensed Content Title	Influence of the β-Sheet Content on the Mechanical Properties of Aggregates during Amyloid Fibrillization
Licensed Content Author	Francesco Simone Ruggeri, Jozef Adamcik, Jae Sun Jeong, et al
Licensed Content Date	Jan 14, 2015
Licensed Content Volume	54
Licensed Content Issue	8
Licensed Content Pages	5
Type of use	Journal/Magazine
Requestor type	Author of this Wiley article
Is the reuse sponsored by or associated with a pharmaceutical or medical products company?	no
Format	Electronic
Portion	Figure/table
Number of figures/tables	1
Original Wiley figure/table number(s)	Figure 2
Will you be translating?	No
Title of new article	Characterising Individual Protein Aggregates by Infrared Nanospectroscopy and Atomic Force Microscopy
Publication the new article is in	JoVE
Publisher of new article	JoVE
Author of new article	Francesco Simone Ruggeri, Tomas Šneideris, Sean Chia, Michele Vendruscolo, Tuomas P. J. Knowles
Expected publication date of new article	Jul 2019
Estimated size of new article (pages)	15
Requestor Location	University of Cambridge Lensfield Road, CB2 1EW Cambridge, CB2 1EW United Kingdom Attn: University of Cambridge

Publisher Tax ID	EU826007151
Total	0.00 EUR

Terms and Conditions

TERMS AND CONDITIONS

This copyrighted material is owned by or exclusively licensed to John Wiley & Sons, Inc. or one of its group companies (each a"Wiley Company") or handled on behalf of a society with which a Wiley Company has exclusive publishing rights in relation to a particular work (collectively "WILEY"). By clicking "accept" in connection with completing this licensing transaction, you agree that the following terms and conditions apply to this transaction (along with the billing and payment terms and conditions established by the Copyright Clearance Center Inc., ("CCC's Billing and Payment terms and conditions"), at the time that you opened your RightsLink account (these are available at any time at http://myaccount.copyright.com).

Terms and Conditions

- The materials you have requested permission to reproduce or reuse (the "Wiley Materials") are protected by copyright.

- You are hereby granted a personal, non-exclusive, non-sub licensable (on a stand-alone basis), non-transferable, worldwide, limited license to reproduce the Wiley Materials for the purpose specified in the licensing process. This license, **and any CONTENT (PDF or image file) purchased as part of your order,** is for a one-time use only and limited to any maximum distribution number specified in the license. The first instance of republication or reuse granted by this license must be completed within two years of the date of the grant of this license (although copies prepared before the end date may be distributed thereafter). The Wiley Materials shall not be used in any other manner or for any other purpose, beyond what is granted in the license. Permission is granted subject to an appropriate acknowledgement given to the author, title of the material/book/journal and the publisher. You shall also duplicate the copyright notice that appears in the Wiley publication in your use of the Wiley Material. Permission is also granted on the understanding that nowhere in the text is a previously published source acknowledged for all or part of this Wiley Material. Any third party content is expressly excluded from this permission.

- With respect to the Wiley Materials, all rights are reserved. Except as expressly granted by the terms of the license, no part of the Wiley Materials may be copied, modified, adapted (except for minor reformatting required by the new Publication), translated, reproduced, transferred or distributed, in any form or by any means, and no derivative works may be made based on the Wiley Materials without the prior permission of the respective copyright owner.**For STM Signatory Publishers clearing permission under the terms of the STM Permissions Guidelines only, the terms of the license are extended to include subsequent editions and for editions in other languages, provided such editions are for the work as a whole in situ and does not involve the separate exploitation of the permitted figures or extracts,** You may not alter, remove or suppress in any manner any copyright, trademark or other notices displayed by the Wiley Materials. You may not license, rent, sell, loan, lease, pledge, offer as security, transfer or assign the Wiley Materials on a stand-alone basis, or any of the rights granted to you hereunder to any other person.

- The Wiley Materials and all of the intellectual property rights therein shall at all times remain the exclusive property of John Wiley & Sons Inc, the Wiley Companies, or their respective licensors, and your interest therein is only that of having possession of and the right to reproduce the Wiley Materials pursuant to Section 2 herein during the continuance of this Agreement. You agree that you own no right, title or interest in or to the Wiley Materials or any of the intellectual property rights therein. You shall have no rights hereunder other than the license as provided for above in Section 2. No right,

license or interest to any trademark, trade name, service mark or other branding ("Marks") of WILEY or its licensors is granted hereunder, and you agree that you shall not assert any such right, license or interest with respect thereto

- NEITHER WILEY NOR ITS LICENSORS MAKES ANY WARRANTY OR REPRESENTATION OF ANY KIND TO YOU OR ANY THIRD PARTY, EXPRESS, IMPLIED OR STATUTORY, WITH RESPECT TO THE MATERIALS OR THE ACCURACY OF ANY INFORMATION CONTAINED IN THE MATERIALS, INCLUDING, WITHOUT LIMITATION, ANY IMPLIED WARRANTY OF MERCHANTABILITY, ACCURACY, SATISFACTORY QUALITY, FITNESS FOR A PARTICULAR PURPOSE, USABILITY, INTEGRATION OR NON-INFRINGEMENT AND ALL SUCH WARRANTIES ARE HEREBY EXCLUDED BY WILEY AND ITS LICENSORS AND WAIVED BY YOU.

- WILEY shall have the right to terminate this Agreement immediately upon breach of this Agreement by you.

- You shall indemnify, defend and hold harmless WILEY, its Licensors and their respective directors, officers, agents and employees, from and against any actual or threatened claims, demands, causes of action or proceedings arising from any breach of this Agreement by you.

- IN NO EVENT SHALL WILEY OR ITS LICENSORS BE LIABLE TO YOU OR ANY OTHER PARTY OR ANY OTHER PERSON OR ENTITY FOR ANY SPECIAL, CONSEQUENTIAL, INCIDENTAL, INDIRECT, EXEMPLARY OR PUNITIVE DAMAGES, HOWEVER CAUSED, ARISING OUT OF OR IN CONNECTION WITH THE DOWNLOADING, PROVISIONING, VIEWING OR USE OF THE MATERIALS REGARDLESS OF THE FORM OF ACTION, WHETHER FOR BREACH OF CONTRACT, BREACH OF WARRANTY, TORT, NEGLIGENCE, INFRINGEMENT OR OTHERWISE (INCLUDING, WITHOUT LIMITATION, DAMAGES BASED ON LOSS OF PROFITS, DATA, FILES, USE, BUSINESS OPPORTUNITY OR CLAIMS OF THIRD PARTIES), AND WHETHER OR NOT THE PARTY HAS BEEN ADVISED OF THE POSSIBILITY OF SUCH DAMAGES. THIS LIMITATION SHALL APPLY NOTWITHSTANDING ANY FAILURE OF ESSENTIAL PURPOSE OF ANY LIMITED REMEDY PROVIDED HEREIN.

- Should any provision of this Agreement be held by a court of competent jurisdiction to be illegal, invalid, or unenforceable, that provision shall be deemed amended to achieve as nearly as possible the same economic effect as the original provision, and the legality, validity and enforceability of the remaining provisions of this Agreement shall not be affected or impaired thereby.

- The failure of either party to enforce any term or condition of this Agreement shall not constitute a waiver of either party's right to enforce each and every term and condition of this Agreement. No breach under this agreement shall be deemed waived or excused by either party unless such waiver or consent is in writing signed by the party granting such waiver or consent. The waiver by or consent of a party to a breach of any provision of this Agreement shall not operate or be construed as a waiver of or consent to any other or subsequent breach by such other party.

- This Agreement may not be assigned (including by operation of law or otherwise) by you without WILEY's prior written consent.

- Any fee required for this permission shall be non-refundable after thirty (30) days from receipt by the CCC.

- These terms and conditions together with CCC's Billing and Payment terms and conditions (which are incorporated herein) form the entire agreement between you and WILEY concerning this licensing transaction and (in the absence of fraud) supersedes all prior agreements and representations of the parties, oral or written. This Agreement may not be amended except in writing signed by both parties. This Agreement shall be binding upon and inure to the benefit of the parties' successors, legal representatives, and authorized assigns.

- In the event of any conflict between your obligations established by these terms and conditions and those established by CCC's Billing and Payment terms and conditions, these terms and conditions shall prevail.

- WILEY expressly reserves all rights not specifically granted in the combination of (i) the license details provided by you and accepted in the course of this licensing transaction, (ii) these terms and conditions and (iii) CCC's Billing and Payment terms and conditions.

- This Agreement will be void if the Type of Use, Format, Circulation, or Requestor Type was misrepresented during the licensing process.

- This Agreement shall be governed by and construed in accordance with the laws of the State of New York, USA, without regards to such state's conflict of law rules. Any legal action, suit or proceeding arising out of or relating to these Terms and Conditions or the breach thereof shall be instituted in a court of competent jurisdiction in New York County in the State of New York in the United States of America and each party hereby consents and submits to the personal jurisdiction of such court, waives any objection to venue in such court and consents to service of process by registered or certified mail, return receipt requested, at the last known address of such party.

WILEY OPEN ACCESS TERMS AND CONDITIONS

Wiley Publishes Open Access Articles in fully Open Access Journals and in Subscription journals offering Online Open. Although most of the fully Open Access journals publish open access articles under the terms of the Creative Commons Attribution (CC BY) License only, the subscription journals and a few of the Open Access Journals offer a choice of Creative Commons Licenses. The license type is clearly identified on the article.

The Creative Commons Attribution License

The Creative Commons Attribution License (CC-BY) allows users to copy, distribute and transmit an article, adapt the article and make commercial use of the article. The CC-BY license permits commercial and non-

Creative Commons Attribution Non-Commercial License

The Creative Commons Attribution Non-Commercial (CC-BY-NC)License permits use, distribution and reproduction in any medium, provided the original work is properly cited and is not used for commercial purposes.(see below)

Creative Commons Attribution-Non-Commercial-NoDerivs License

The Creative Commons Attribution Non-Commercial-NoDerivs License (CC-BY-NC-ND) permits use, distribution and reproduction in any medium, provided the original work is properly cited, is not used for commercial purposes and no modifications or adaptations are made. (see below)

Use by commercial "for-profit" organizations

Use of Wiley Open Access articles for commercial, promotional, or marketing purposes requires further explicit permission from Wiley and will be subject to a fee.

Further details can be found on Wiley Online Library

http://olabout.wiley.com/WileyCDA/Section/id-410895.html

Other Terms and Conditions:

v1.10 Last updated September 2015

Questions? customercare@copyright.com or +1-855-239-3415 (toll free in the US) or +1-978-646-2777.

Nanoscale studies link amyloid maturity with polyglutamine diseases onset

F. S. Ruggeri , S.Vieweg, U. Cendrowska, G. Longo, A. Chiki, H.A. Lashuel & G. Dietler

https://doi.org/10.1038/srep31155